RELATIONSHIPS AMONG KEY

REACTOR SYSTEMS DESIGN VARIABLES

Professor Neil Todreas

TABLE OF CONTENTS

The term "reactor systems" is employed versus "reactor" to emphasize that the production of electricity by nuclear fission employs a reactor operating in a fuel cycle. The fuel cycle introduces front and back end fuel handling operations which bracket the in-reactor fuel residence period during which the fuel is fissioned to produce the reactor output.

The selection of the reactor design parameters is an interdisciplinary task involving detailed analysis in the area of neutronics, materials, behavior and structural mechanics, thermal science, control and risk assessment. However, the key characteristics of the reactor core can be related and established by a small number of relations best illustrated in the context of their impact on the final cost of the generated electricity.

1.0 KEY DESIGN PARAMETERS ARISING FROM ECONOMIC ASSESSMENT

The methodology typically employed for the cost assessment of electricity production is the lifetime levelized cost method. This method determines the cost of electricity per unit of energy delivered by the power plant as the continuous stream of revenues over the useful life of the expenditures (i.e. the fuel lifetime in this case of fuel cycle expenditures) that is required in order to recover the expenditures themselves. It is also called the levelized busbar unit cost of electricity, to reflect that only expenses up to the transmission line are included. Thus, the term "levelized" means that the costs, originally incurred at certain discrete times, are "distributed continuously" during the fuel in-core residence period and recovered through the corresponding continuous stream of revenues from the sale of electricity. This method permits a single valued numerical comparison of alternatives having vastly different cash flow histories.

There are several ways to implement this methodology particularly for the fuel cost component. The work of Saccheri, 2003 and Shuffler, 2004 illustrate applications of the basic methodology for the PWR cores. The work of Wang, 2003, for the seed and blanket fuel cycles in PWRs, illustrates a more complex application for fuel cycle costs, because the operating cycle lengths for fuel assemblies in the seed and blanket core regions differ. Shuffler's approach which is based on that originally proposed by Ssaccheri, 2003, is presented in Appendix A for illustration. Here we proceed directly to the results of Driscoll, 2005, which are simplified expressions for the

three cost components – capital, operating and maintenance and fuel - whose sum is the Lifetime-Levelized Busbar Cost of Electric Energy. These results (with some transformations in symbols and units) are presented in equations 1 through 3 and are based on these three factors:

- The cost of money ("interest paid on borrowed funds"), x, is given by the weighted average of the expected rates of return on debt (bonds) and equity (stocks)

- Future expenses are escalated at rate, y, per year.

- The plant capital cost at time zero is computed from an overnight cost (i.e., hypothetical instantaneous construction), corrected for escalation and interest paid on borrowed funds over a construction period starting c years before operation $\left(\dfrac{I}{K}\right)_{-c}$.

The Lifetime-Levelized Busbar Cost of Electrical Energy, calculated for average values of nuclear fuel unit costs and a typical cash flow history for PWRs (from Driscoll, 2005), $\bar{c}_{lev}$, in mills per kilowatt hour electric (10 mills equal 1 cent) is the sum of:

Capital-Related Costs:

$$\frac{1000\phi}{8,766L}\left(\frac{I}{K}\right)_{-c}\left[1+\frac{x+y}{2}\right]^{c} \tag{1}$$

Plus Operating and Maintenance (O&M) Costs:

$$\frac{1000}{8,766L}\left(\frac{O}{K}\right)_{O}\left[1+\frac{yT_{plant}}{2}\right] \tag{2}$$

Plus Fuel Costs:

$$\left[\frac{1}{24}\frac{F_{o}}{\eta\,Bu_{d}}\right]\left[1+\frac{yT_{plant}}{2}\right] \tag{3a}$$

where:

		Typical LWR Value[†]
L	plant capacity factor: actual energy output $\div$ energy if always at 100% rated power	0.90
ϕ	annual fixed charge rate (i.e.,, effective "mortgage" rate) approximately equal to $x/(1-\tau)$ where x is the discount rate,, and τ is the tax fraction (0.4)	0.125/yr
x	$(1-\tau)b\,r_b + (1-b)r_s$ in which b is the fraction of capital raised selling bonds (debt fraction), and r_b is the annualized rate of return on bonds,, while r_s is the return on stock (equity)	0.078/yr
$\left(\dfrac{I}{K}\right)_{-c}$	overnight specific capital cost of plant,, as of the start of construction, dollars per kilowatt: cost if it could be constructed instantaneously c years before startup in nominal dollars without inflation or escalation,	$1,500/kWe
y	annual rate of monetary inflation (or price escalation,, if different)	0.03/yr
c	time required to construct plant, years,	4 yrs
T_{plant}	prescribed useful life of plant, years	40 yrs
$\left(\dfrac{O}{K}\right)_O$	specific operating and maintenance cost as of start of operation, dollars per kilowatt per year	$114/kWe yr
η	plant thermodynamic efficiency, net kilowatts electricity produced per kilowatt of thermal energy consumed,	0.33
F_o	net unit cost of nuclear fuel,, first steady-state reload batch,, dollars per kilogram of uranium; including financing and waste disposal charges,, as of start of plant operation,	$2,000/kg
Bu_d	burnup of discharged nuclear fuel, megawatt days per kilogram of heavy metal	45 Mwd/kg

Note that these costs represent only the cost of generating the electricity (i.e., excluding transmission and distribution). These costs are lifetime-average (i.e., "levelized") costs for a new plant starting operations today. For instance, for a light water reactor (LWR) nuclear power plant, using the representative values cited above:

$$
\begin{array}{ccccccccc}
 & & \text{Capital} & & \text{O\&M} & & \text{Fuel}^{\ddagger} & & \\
\bar{c}_{lev} & = & 31 & + & 24.5 & + & 9 & = & 64.5 \text{ mills/kW-hre}
\end{array}
$$

The fuel discharge burnup for an in-core residence time, T_{res}, can be expressed as

$$Bu_d = 0.365 q_{sp}\, L\, T_{res} \qquad\qquad (4)$$

where

[†] Taken for case with plausible cost improvements (Chapter 1) of MIT Study of the Future of Nuclear Power, July 2003
[‡] This fuel cycle cost is higher than an LWR in operation today, because it accounts for price escalation at 3%/yr.

Bu_d	fuel discharge burnup	$\dfrac{Mwd}{kg}$
q_{sp}	specific power	$\dfrac{kWth}{kg_{HM}}$
T_{res}	fuel in-core residence time	yrs
0.365	conversion factor	days/yrx10^{-3}

The relationship between the parameters of Eqn. 4 is illustrated in Fig. 1 for a plant capacity factor of 90%.
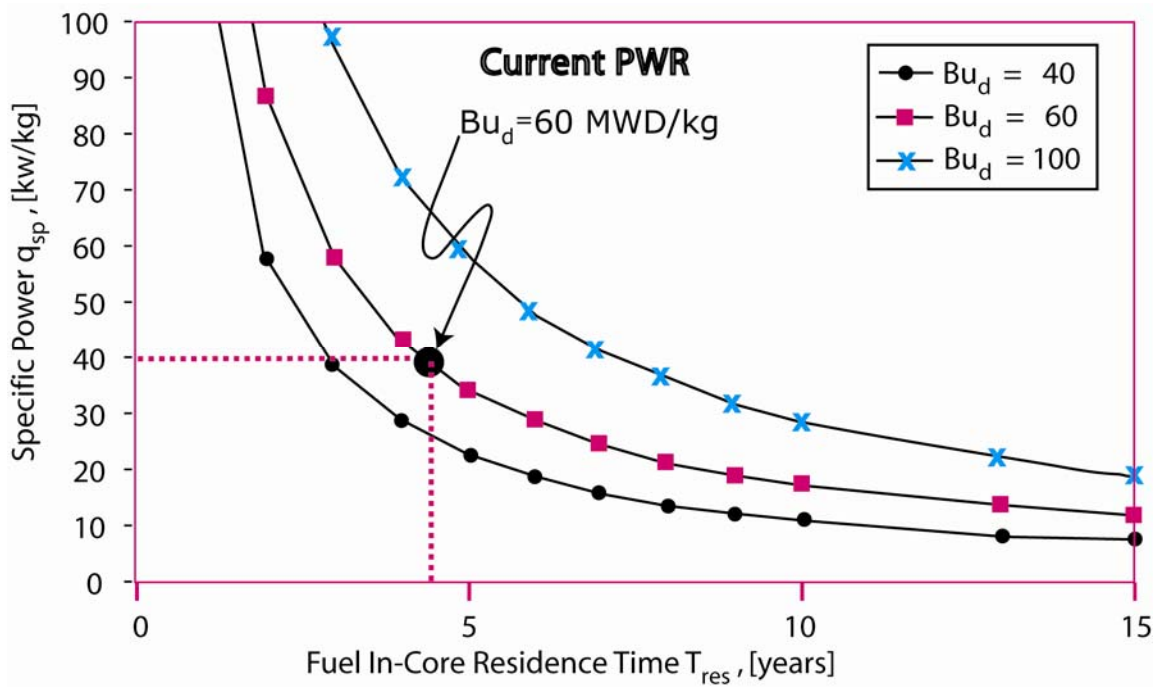

Figure 1. The Specific Power Fuel Residence Time Tradeoff for Plant Capacity Factor of 90% (from Saccheri, 2002)

Using Equation 4, the fuel cycle cost can also be expressed as:

$$\frac{1}{24}\ \frac{F_o}{0.365 q_{sp} L\ T_{res} \eta}\ \left[1 + \frac{y T_{plant}}{2}\right] \qquad (3b)$$

2.0   CORE DESIGN IMPLICATIONS FOR MINIMIZING COE

Let us focus on Equations (1) through (3) to highlight the implications for core design in minimizing the lifetime levelized unit cost of electricity, $\bar{c}_{lev}$. Hence our design parameters of importance are $q_{sp,}\ Bu_d,\eta,L,T_{res}$ and T_{plant}.

From these equations we see that costs are minimized as the following parameters are increased and unit present value costs for fuel, capital and O & M are decreased

q_{sp},η,L,T_{res} and Bu_d

The effect of longer T_{plant} reducing cost is masked by the approximations made in obtaining Equations 1 though 3.

Tradeoffs between neutronics, core thermal hydraulic, thermodynamic power cycle, fuel performance as well as operations and maintenance practice dictate the achievable selection of values for these parameters. For the typical operating PWR and the most prominent version of the Generation IV gas fast reactor (GFR)[§] such values are summarized in Table 1.

Table 1. PWR and GFR core parameters

Parameter	Symbol	PWR (Romano et al, 2005)	GFR (GFR023, Feb. 2005)
Core Power [MWth]	Q_{th}	3000	2400
Net Electric Output [MWe]	Q_e	1,000	600-1200
Fuel		UO_2	UC-SiC Cercer*** Plates, Blocks or Rods
Enrichment [wt%]	$\in$	4.2	15.5/18.5(TRU)
HM Loading in Core [MT]	M_{HM}	77.2	
Specific Power [kWth/kg$_{HM}$]	q_{sp}	38	38
Core Power Density [kWth / l]	q_{PD}	104.5	100
Number of Batches	n	3	?
Operating Cycle Length or Refueling Interval [years]	T_c	1.5	?
Capacity Factor	L	0.9	?
Coolant		Water	He or CO_2

[§] The GFR design is being evolved. The large plant GFR design is cited in this note.

			?
Uranium Destruction[**] Rate [MT / GWe / yr]		1.28	
TRU Production Rate [MT / GWe / yr]		0.28	?
TRU / HM Fraction in Discharged Fuel[%]		1.28	?

[*]   Weight percent content of TRU
[**]   Includes all uranium isotopes, destruction by both capture and fission
[***]   UN and $U^{15}N$ are also candidates

     We will now proceed to provide relationships between these parameters and others used by the individual disciplinary areas, e.g. reactor physics, thermal hydraulics to execute the core design. In the process we will also identify relationships to the multiple additional parameters used by these individual disciplines to express performance.

2.1   Discharge Burnup, Bu_d

     Discharge burnup is constrained by both fuel pin mechanical performance and reactivity limits. Fuel pin mechanical performance is assessed by use of complex analysis tools which predict achievable burnup subject to limits of fuel pin internal pressure, total clad strain and coolant side oxidation which for a PWR are typically 2500 psia, 1% and 4 mils for steady state operation respectively. Reactivity-limited burnup in LWRs depends principally on fuel enrichment which currently is licensed only to 5 w/o U^{235}. Achievable burnup is conveniently illustrated in terms of moderation effect expressed as the hydrogen to heavy metal ratio $\dfrac{H}{HM}$ and the weight % U^{235} in the U fuel, the enrichment, $\in$ %. This relationship is illustrated in Figure 2 for a single batch loading where typical PWR conditions are highlighted. Similar relationships for various fertile/fissile fuel combinations are shown in Figure 3.
     The current fuel performance constrained discharge burnup limits for oxide fuels in light water reactors depend on the specific portion of the fuel considered. These limits are placed on various portions of the fuel in a core load by different counties. Further they vary with fuel type e.g. UO_2 versus MOX fuel. These limits are given in Table 2.

Table 2. LWR Fuel Performance Constrained Discharge Burnup Limits – (Taken from NEA/CSNI/R (2003) 10, July 2003, "Fuel Safety Criteria in NEA Member Countries")
all MWD/ kg$_{HM}$

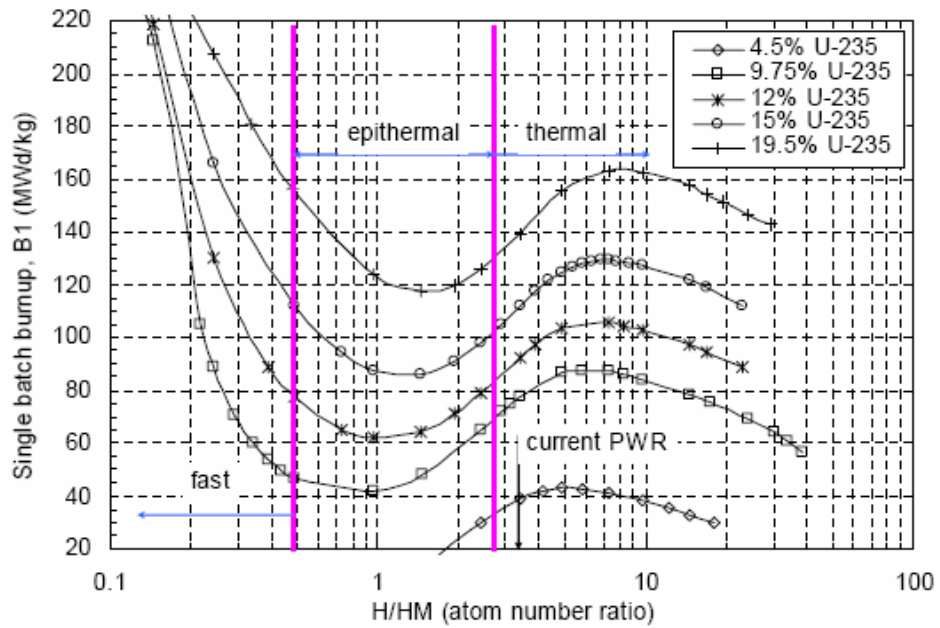|	Country	UO_2	MOX
Average Assembly	Finland/France/Japan/Belgium	45/54/48-55/55	None/None/40-45/50
Axial Average of Peak Fuel Pin	USA	62	None
Peak Pellet	UK	55	None

Figure 2. Achievable Discharge Burnup for Enriched Uranium Dioxide Fuel for Poison-Free, Reactivity Limited, Batch Reload Conditions (taken from Xu, 2003)
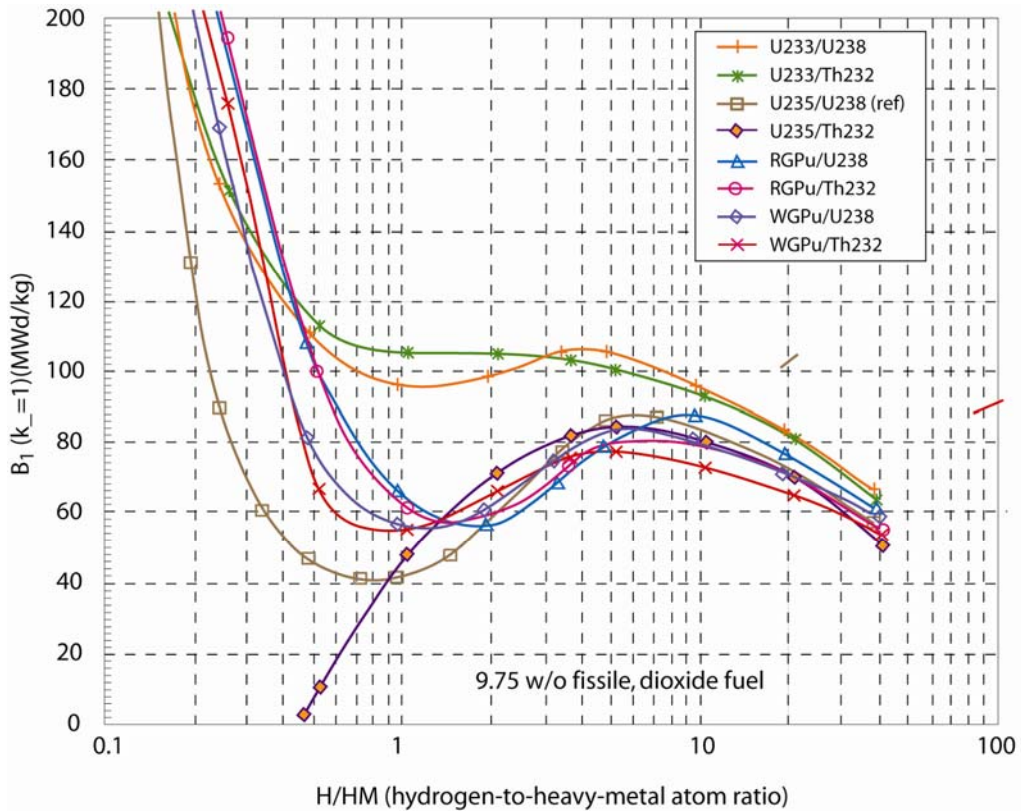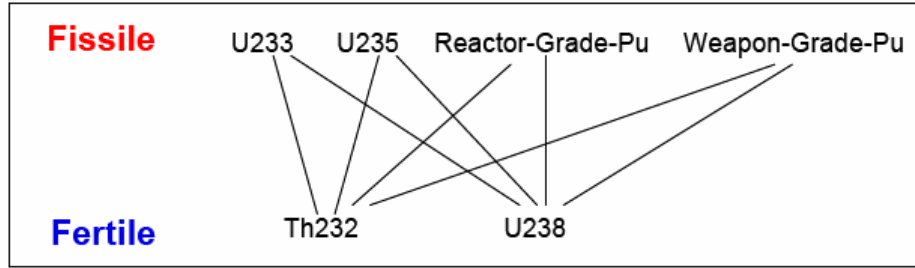
Figure 3. Achievable Discharge Burnup for Fuels of Various Fertile/Fissile Combinations (taken from Xu, 2003)

The ratio $\dfrac{H}{HM}$ can be related to the geometric parameter, the fuel array pitch to rod diameter ratio, $\dfrac{P}{D}$ which is used principally in the thermal/hydraulic analysis. However, the $\dfrac{P}{D}$ value corresponding to a given $\dfrac{H}{HM}$ depends on the array geometry, the most important options being the square and the triangular arrangements, as discussed in Section 2.5. Further variation exists for the triangular arrangement between use of grid and wire spacers.

The principle relations for $\dfrac{H}{HM}$ and $\dfrac{P}{D}$ are presented below and evaluated for various fuels in Appendix B.

In general, for fuels that are hydrogen free, for example the standard UO_2 fuel form:

$$\frac{H}{HM} = 2\left(\frac{M_{HM}}{M_{H_2O}}\right)\left(\frac{\rho_{H_2O}}{\rho_{HM}}\right)\left(\frac{V_{H_2O}}{V_{HM}}\right) \tag{5}$$

For the triangular lattice:

$$\frac{H}{D} = \left(\frac{M_{HM}}{M_{H_2O}}\right)\left(\frac{\rho_{H_2O}}{\rho_{HM}}\right)\left(\frac{\dfrac{4\sqrt{3}\,P^2}{2\pi} - D_{ROD}^2}{d_{Pellet}^2}\right) \tag{6a}$$

If :   a) gap thickness $= 1\%$ of the pellet diameter
and
        b) clad thickness $= 7\%$ of the pellet diameter
        then $D_{ROD} = 1.16\ d_{Pellet}$

Then:

$$\frac{H}{HM} = 2\left(\frac{M_{HM}}{M_{H_2O}}\right)\left(\frac{\rho_{H_2O}}{\rho_{HM}}\right)(1.16)^2\left[\frac{2\sqrt{3}}{\pi}\left(\frac{P}{D_{ROD}}\right)^2 - 1\right] \tag{7a}$$

Writing Equation (6) explicitly in terms of P/D yields:

$$\frac{p}{D} = \frac{p}{D_{ROD}} = \sqrt{\left[\frac{1}{2}\frac{H}{HM}\left(\frac{M_{HM}}{M_{H_2O}}\right)\left(\frac{\rho_{H_2O}}{\rho_{HM}}\right) + (1.16)^2\right]\frac{\pi}{2\sqrt{3}(1.16)^2}} \tag{8a}$$

For the square lattice the analogous equations are:

$$\frac{H}{HM} = 2\left(\frac{M_{HM}}{M_{H_2O}}\right)\left(\frac{\rho_{H_2O}}{\rho_{HM}}\right)\left(\frac{\dfrac{4P^2}{2\pi} - D_{ROD}^2}{d_{Pellet}^2}\right) \tag{6b}$$

If :   a) gap thickness $= 1\%$ of the pellet diameter
and
        b) clad thickness $= 7\%$ of the pellet diameter
        then $D_{ROD} = 1.16\ d_{Pellet}$

10

then,

$$\frac{H}{HM} = 2\left(\frac{M_{HM}}{M_{H_2O}}\right)\left(\frac{\rho_{H_2O}}{\rho_{HM}}\right)(1.16)^2\left[\frac{4}{\pi}\left(\frac{P}{D_{ROD}}\right)^2 - 1\right]$$ (7b)

and :

$$\frac{p}{D} = \frac{p}{D_{ROD}} = \sqrt{\left[\frac{1}{2}\frac{H}{HM}\left(\frac{M_{HM}}{M_{H_2O}}\right)\left(\frac{\rho_{H_2O}}{\rho_{HM}}\right) + (1.16)^2\right]\frac{\pi}{4(1.16)^2}}$$ (8b)

Finally, from Equations 8a and 8b it follows that the pitches of the square and triangular arrays for equal *H/HM* and rod diameter are related as

$$P_{tri} = 1.0746 P_{sq}$$ (9)

For LWR oxide fuel let us evaluate the needed ratios of M_{H_2O}/M_{HM} and ρ_{HM}/ρ_{H_2O} for equations 8a and 8b.

Table 3.

U^{235} enrichment	3.95 [%]
Atomic Mass of HM	237.58 [a.m.u]
Atomic Mass of H$_2$O	18 [a.m.u]
M_{HM}/M_{H_2O}	13.20
UO$_2$ Theoretical density (TD)	10.97 [g/cm^3]
% of TD	0.95 [-]
HM actual density	9.1844 [g/cm^3]
H$_2$O actual density (300 C)	0.705 [g/cm^3]
ρ_{H_2O}/ρ_{HM}	0.07676

Hence for LWR oxide fuel from equations 8a and 8b for *H/HM* = 1.29, the resultant triangular and square fuel array *P/D* ratios are 1.156 and 1.075 respectively.

Figure 5 illustrates the above relations for UO$_2$ as well as for the zirconium hydride fuel form, an alternate being explored to increase core power in LWR service by virtue of its inherent characteristic of providing a substantial degree of moderation in the fuel itself thereby reducing the needed water coolant volume fraction for neutronic performance.
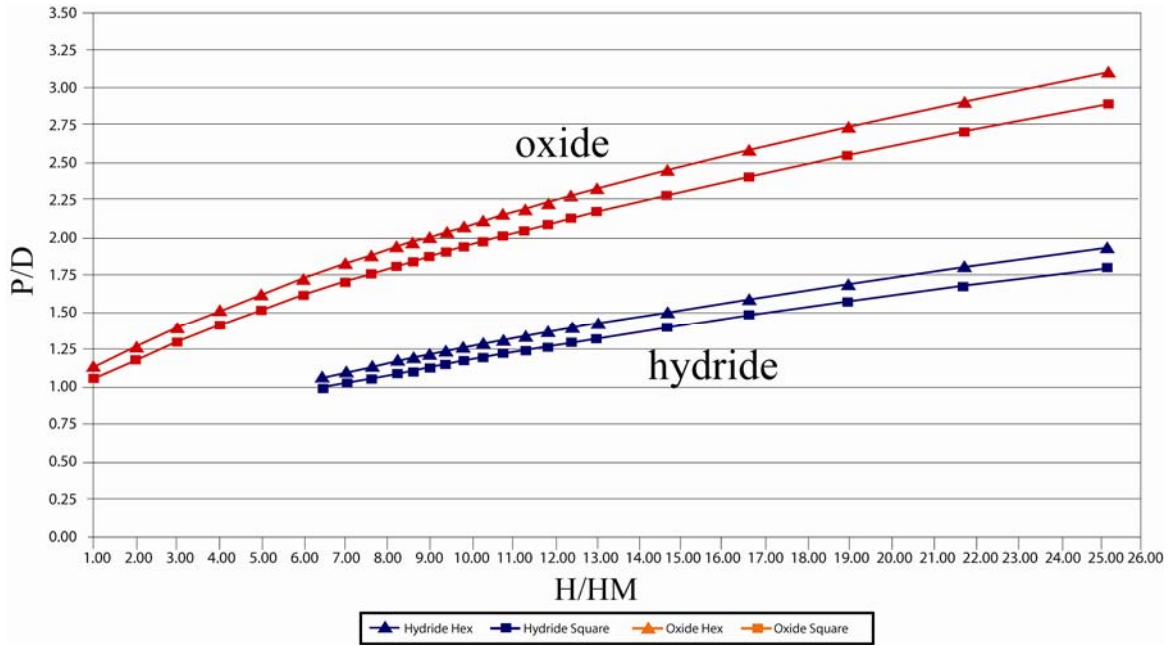
Figure 5. P/D vs H/HM for Square and Hexagonal arrays of UZrH1.6 and UO2

2.2 Fuel in-core residence Time, T_{res}

Achievement of discharge burnup in one operating cycle requires excessive enrichment as well as results in uneconomical discharge of peripheral fuel assemblies at considerable lower burnup, because the leakage lowers the neutron flux at the periphery and determines the core radial (and axial) power profiles. Hence, multi-batch fuel management schemes are used which shuffle fuel within the core as well as add fresh fuel to $1/n^{th}$ of the core at refueling outages. Discharge burnup Bu_d, operating cycle burnup Bu_c and single batch ($n=1$) loaded core burnup Bu_1 are related [**] as follows,

$$Bu_d = n\ Bu_c = \frac{2n}{n+1} Bu_1 \tag{10}$$

where n is the number of fuel batches. Note that in general, n need not be an integer.

The corresponding relevant time periods are related as

$$T_{res} = n\ T_c \tag{11}$$

where T_c is the operating cycle length or refueling interval.

The fuel (in-core residence time) and hence the number of batches is also limited by allowable coolant side oxidation of the fuel clad and fast fluence exposure to the clad and assembly structures.

[**] Based on linear reactivity theory from M.J. Driscoll, T.J. Downar and E.E. Pilat, "The Linear Reactivity Model for Nuclear Fuel Management", American Nuclear Society, 1990

12

It has been found by Xu , 2003 that while single-batch burnup depends on many variables, it can be related to core-average reload fuel enrichment, $\in_p$ from 3 w/o to 20 w/o, the upper limit normally taken as proliferation resistant as

$$Bu_1 = 64.6\sqrt{\in_p +13.4} - 240.4 \qquad\qquad MWd/kg \qquad\qquad (12)$$

(multiply by 1000 to obtain MWd/MTU, the unit plotted in Figure 6)

Hence, solving equations (4),(10), (11) and (12) simultaneously we can obtain the useful map of Fig. 5 relating discharge burnup to operating cycle length for a typical PWR. Note that the specific power and capacity factor in equation 4 have been fixed at prescribed values cited in Figure 5.

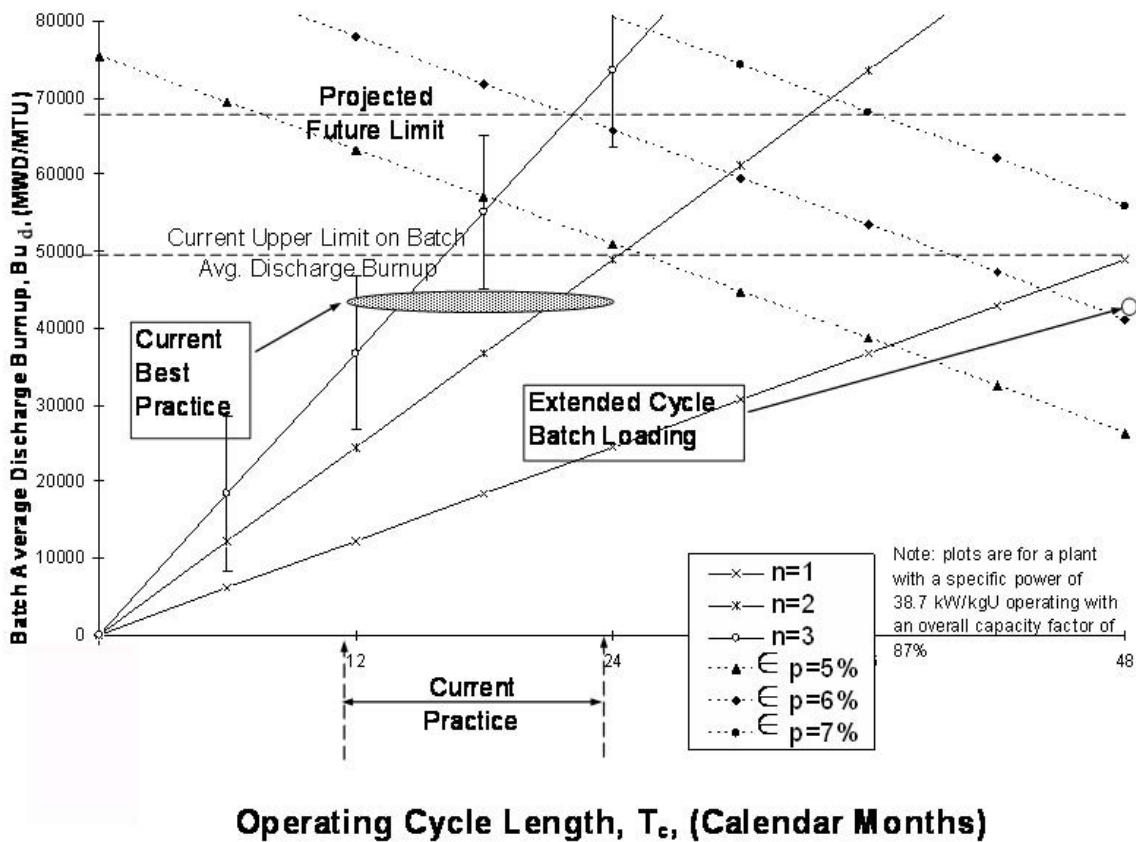**Figure 6. Burnup-Cycle Length Map for a Representative PWR** (from Handwerk, 1997)

2.3   Plant Capacity Factor, L_C

Considerable management attention is paid to enhancement of the plant capacity factor throughout the operating fleet. Central has been the control of the duration of planned plant shutdowns for refueling and maintenance and unplanned shutdowns from unplanned outage extensions and forced outages.

13

Figure 7 is an illustration of the actual power history of a hypothetical plant during an operating cycle which encompasses the period from successive startups after shutdown to perform core refueling. Figure 1 is typically called a plant skyline reflective of the imagery of the illustration. As shown the power losses can be partial load reductions or full shutdowns – some planned, some unplanned and some not under control of the plant operator. Also shown is a power coastdown period prior to the refueling period at the end of the cycle.

Figure 7
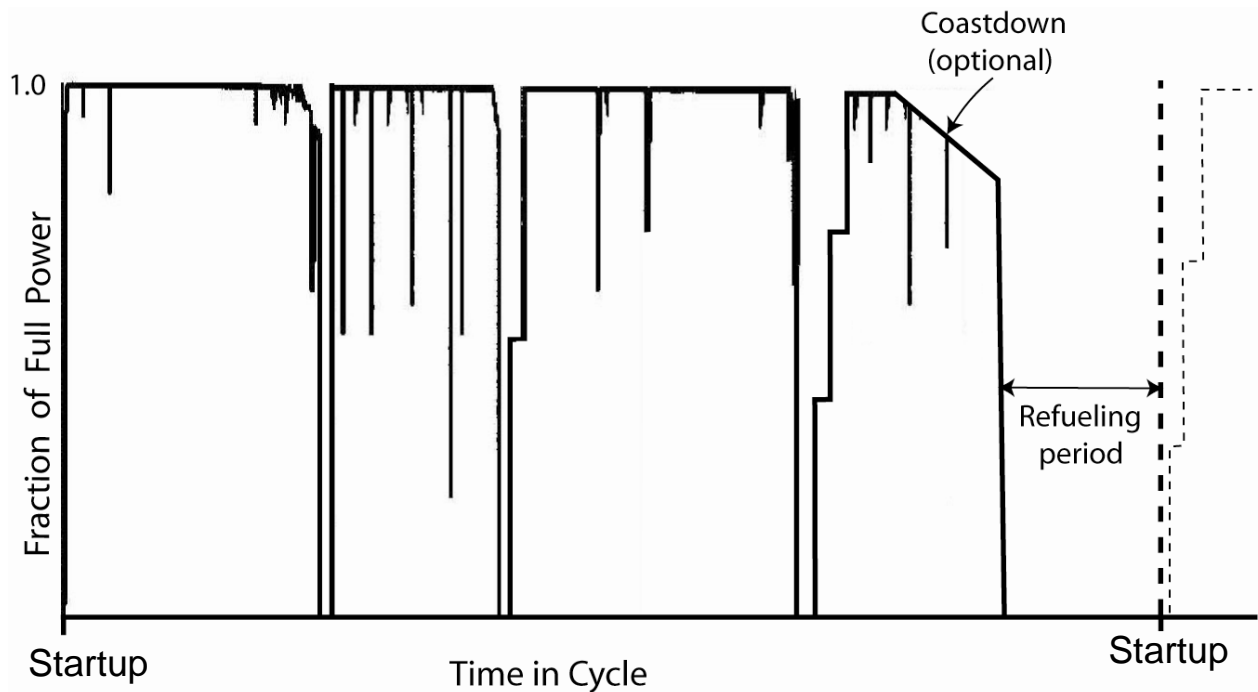
Various parameters have been defined to characterize this operational history, all of which report some averaged fraction of full power operation. They differ principally in which components of operating power losses they account for. Here we will focus first upon the plan capacity factor, L_C, and plant unit capability factor, L_{CB}. Plant availability, L_A, will be introduced later.[*]

The plant capacity factor, L_C, accounts for downtime from all causes, i.e. planned and unplanned outages due to causes under plant management control as well as energy losses not considered to be under the control of plant management such as lack of demand, grid instability or failure, fuel coastdowns, environmental limitations and seasonal variations. Plant unit capability factor, L_{CB}, in contrast, accounts only for downtime from causes within the plant control. Table 4 illustrates these categories of operation losses.

---

[*] Capacity and capability factors are the two most commonly cited parameters. They plus availability, however, do not exhaust the complete list of parameters used by various or industry organizations which report and monitor nuclear plant operational performance.

Table 4   Categories of Operating Losses in an Operating Cycle

Outages within Operator Control		Outages outside Operator Control
Unplanned Outages (UO) yield Unplanned Energy Loss (DEL)	Planned Outages (PO) yield Planned Energy Loss (PEL)	Idle Outages (I) yield Energy Loss from Idle Periods (IEL)

Hence plant capacity factor is

$$L_C = \frac{\text{Reference Energy Generation Minus All Energy Losses}}{\text{Reference Energy Generation}}$$

$$= \frac{\text{Actual Generation}}{\text{Reference Energy Generation}} \tag{13}$$

$$= \frac{REG - UEL - PEL - IEL}{REG} = \frac{AG}{REG}$$

while the plant unit capability factor, L_{CB}, is

$$L_{CB} = \frac{\text{Reference Energy Generation Minus Energy Losses within Operator Control}}{\text{Reference Energy Generation}}$$

$$= \frac{REG - UEL - PEL}{REG} \tag{14}$$

where AG = Energy Generation over a Selected Time Period

REG = Reference Energy Generation Equal to the Selected Time Period × Plant
Reference Power Rating

UEL = Unplanned Energy Loss Summed over All Occurrences

PEL = Planned Energy Loss Summed over All Occurrences

IEL = Energy Loss from Idle Periods outside Plant Operator Control over All Occurrences

Reference energy generation, REG, is the energy that could be produced if the unit were operated continuously at full power under reference ambient conditions throughout the given period. Reference ambient conditions are environmental conditions representative of the annual mean (or typical) ambient conditions for the unit.

Hence

$$\frac{L_C}{L_{CB}} = \frac{REG - UEL - PEL - IEL}{REG - UEL - PEL}$$

$$= \frac{AG}{REG - UEL - PEL}$$

(15)

Note that all terms are in energy units typically expressed in kWhrs. The times associated with downtimes are real times during which power losses have occurred.

Hence we desire to transform these results to effective times (for operations or loss) at full power so that corresponding times (e.g. downtime due to a series of forced load reductions) are equally weighted and therefore can be added. We express effective time in terms of actual time and power rating as follows:

$$T_{eff} \, P_{rated} = \sum_i T_{ACT} \, (P_{rated} - P_{actual\,operating})$$

(16)

where $(P_{rated} - P_{actual\,operating})$ is the power lost for the actual time T_{ACT} for occurrence i.

So if we are interested in forced outage loss, i.e. the effective time for loss of full power,

$$T_{FO} = \frac{\sum_i T_{ACT}(P_{rated} - P_{actual\,operating})}{P_{rated}}$$

(17)

Table 5 illustrates the effective time periods for operation, EFPP, unplanned outages, T_{EO} & $T_{FO,}$ planned outages, T_{RO} & T_{MO}, and idle time, T_I.

Table 5   Time Periods in an Operating Cycle

Operation	Outages within Operator Control				Outages outside Operator Control
At Power	Unplanned Outages (UO) T_{UO}		Planned Outages (PO) T_{PO}		Idle Outages (I)
Effective Full Power Period, EFPP	Outage Extension (EO) T_{EO}	Forced Outage (FO) T_{FO}	Refueling Outage (RO) T_{RO}	Maintenance Outage (MO) T_{MO}	T_I

Now we can express plant capacity factor and the unit capability factor in terms of EFPP (Effective Full Power Period), T_{CB} (Capability Factor Equivalent Cycle Length), and T_C (Cycle Length).   Figure 8 illustrates these relationships where the terms L_A, plant availability, and T_A, availability time have been introduced. Note in particular, as discussed later, that the individual times T_{PO}, T_{UO} and T_I are illustrated only as their sum which equals $T_C - $ EFPP.

Figure 8   Plant Operating Characteristics
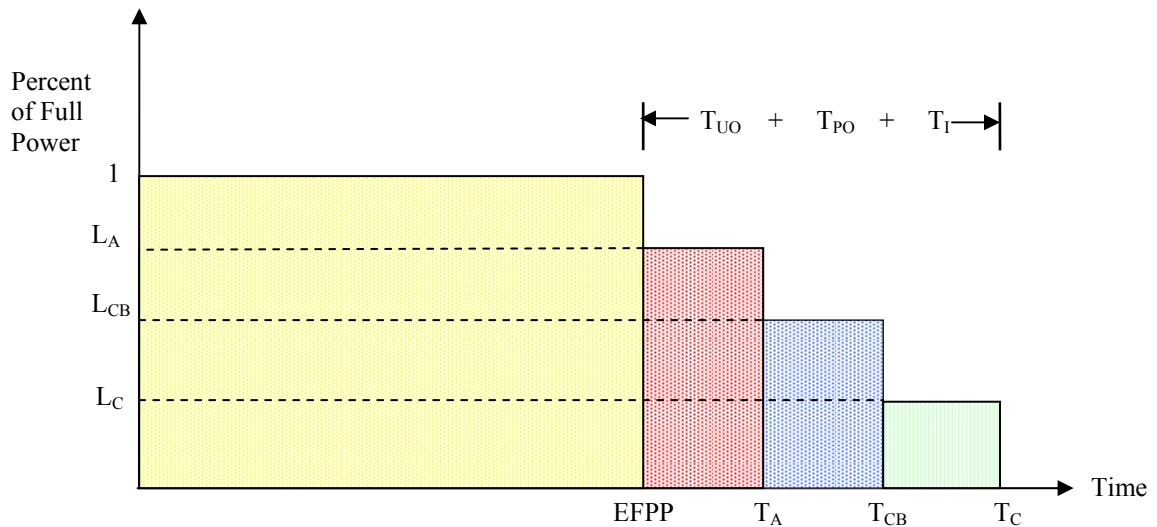
The enclosed areas in this figure are energy quantities since the ordinate is % full power and the abscissa is time. Since the actual energy generated over a cycle, T_C, is fixed from the energy balance of Figure 8, we can write

$$100\% \ \text{EFPP} = L_A T_A = L_{CB} T_{CB} = L_C T_C \tag{18}$$

17

Hence

$$\frac{L_C}{L_{CB}} = \frac{T_{CB}}{T_C}$$ (18a)

Now following equations 6 and 1, we can express the plant capacity factor, L_C, as

$$L_C = \frac{1 \cdot EFPP}{T_C} = \frac{T_C - T_I - T_{PO} - T_{UO}}{T_C}$$ (19)

Similarly from equation 6, we can express the plant capability factor, L_{CB}, as

$$L_{CB} = \frac{1 \cdot EFPP}{T_{CB}}$$ (18b)

and expressing equation 2 in similar terms

$$L_{CB} = \frac{T_C - T_{PO} - T_{UO}}{T_C}$$ (20)

For simplicity let us next take T_{EO} and T_{MO} equal to zero. We can now express plant capacity factor, L_C and plant capability factor, L_{CB} versus cycle length, T_C, in terms of the commonly used variables T_C, T_{RO}, T_I and FLR (forced loss rate which is defined below). Hence from the definitions of Figure 8

$$T_{PO} = T_{RO} + T_{MO} \Rightarrow T_{RO}$$
and
$$T_{UO} = T_{EO} + T_{FO} \Rightarrow T_{FO}$$

Now T_{FO} is typically expressed in terms of the forced loss rate, FLR, defined as[*]

$$FLR = \frac{\text{Unplanned Forced Energy Losses}}{\text{Reference Energy Generation} - (\text{Planned Plus Unplanned Outage Extension Energy Losses})}$$ (21)

Using the effective times introduced earlier we obtain

$$FLR = \frac{T_{FO}}{T_C - T_{PO} - T_{EO}}$$ (22)

---

[*] This indicator has been constructed by the industry to monitor progress in minimizing outage time and power reductions that result from unplanned equipment failures, human errors, or other conditions during the operating period. The operating period which is the denominator of the definition has therefore been defined to exclude planned outages and their possible unplanned extensions.

For our assumption that T_{EO} and T_{MO} are zero, equation 10 reduces to

$$FLR = \frac{T_{FO}}{T_C - T_{RO}} \tag{23}$$

Hence T_{FO} is available from equation 23 in terms of the assumed known parameters FLR, T_C and T_{RO} as:

$$T_{FO} = FLR\,(T_C - T_{RO}) \tag{24}$$

Now plant capacity factor can be expressed from equations 19 and 24 as

$$L_C = \frac{T_C - T_I - T_{RO} - T_{FO}}{T_C} = \frac{(T_C - T_{RO})(1 - FLR) - T_I}{T_C} \tag{25}$$

Similarly, the plant capability factor, L_{CB}, can be expressed from equations 20 and 24 as

$$L_{CB} = \frac{T_C - T_{RO} - T_{FO}}{T_C} = \left[\frac{T_C - T_{RO}}{T_C} \right](1 - FLR) \tag{26}$$

If, for example, a 30 day idle time, T_I, is assumed along with a 30 day refueling outage length, T_{RO}, the plant capacity factor, L_C, and the plant capability factor, L_{CB}, can be calculated for given values of FLR. The results are displayed in Figure 9. Note that the values of capability and capacity factor as illustrated in Figure 9 differ for the same values of T_{RO} and FLR by:

$$\frac{L_C}{L_{CB}} = 1 - \frac{T_I}{(T_C - T_{RO})(1 - FLR)} \tag{27}$$

which is obtained by dividing equation 13 by 14. From Figure 9 at assumed values of 5% FLR, T_I =30 days, T_{RO} = 30 days and T_C = 24 months, the capability factor is 0.91, while the capacity factor is lower at 0.87. The ratio is 0.95 as equation 27 confirms.

**Figure 9   Effect of Cycle Length on Plant Operating Factors
(assuming a 30 day refueling outage length, T_{RO}) and 30 Day Idle
Time Period, T_I, outside the Plant Operator's Control**
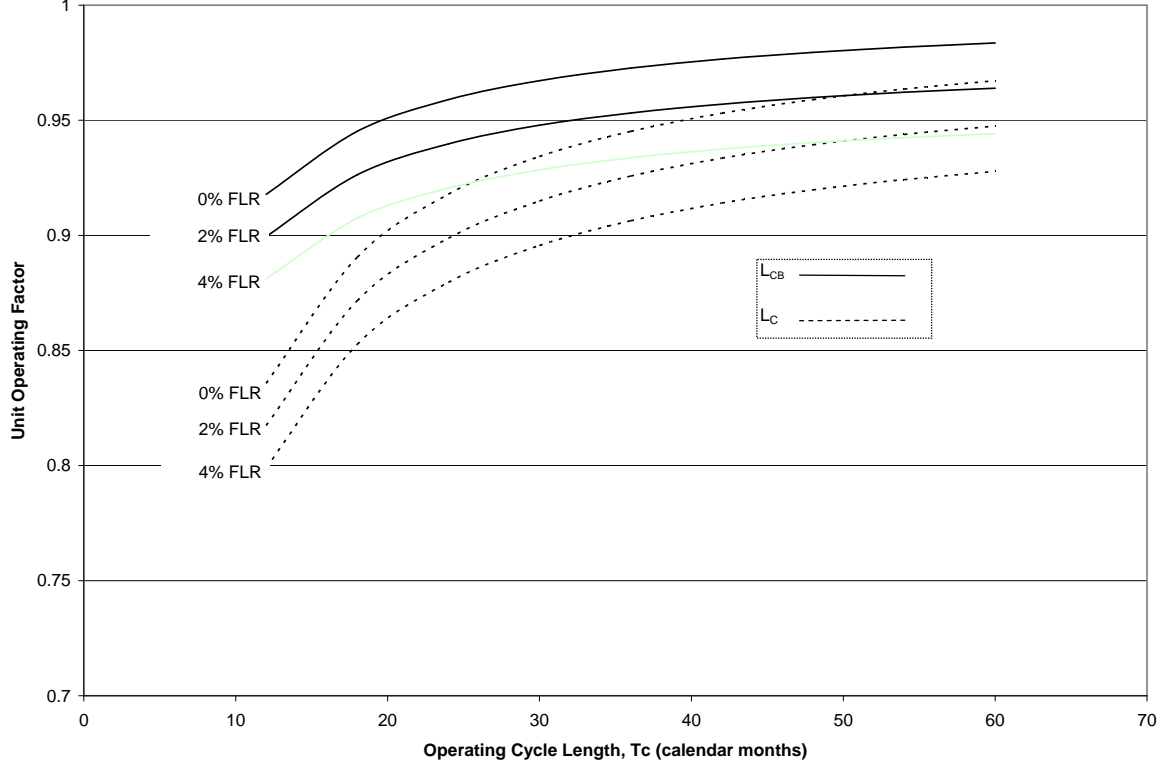
We conclude this Section by elaborating Figure 8 to express the differences among the times EFPP, T_{CB}, T_A and T_C in terms of the outage times (i.e. T_{RO}, T_{FO}, and T_I). These relations are not simple because the definition of capability factor, L_{CB}, has adopted T_C as its reference time, and availability factor, L_A, uses T_C - T_{RO}.

First from equation 15 and 6a we express the difference between T_C and T_{CB} as

$$T_C - T_{CB} = T_I \left[\frac{T_C}{(T_C - T_{RO})(1 - FLR)} \right] \tag{28a}$$

And by reintroducing equation 11, we can define T_I*, the difference between T_C and T_{CB}

$$T_C - T_{CB} = T_I \left[\frac{T_C}{T_C - T_{RO} - T_{FO}} \right] \equiv T_I * \tag{28b}$$

The difference between T_{CB} and T_A is obtained by first expressing T_A from equation 18 as

20

$$\frac{T_A}{T_C} = \frac{L_C}{L_A} \qquad (18c)$$

The plant availability factor, L_A, is defined as the power produced over the operating cycle plus that which could have been produced at full power over the idle time, T_I, which is not in the operator's control divided by the cycle length minus planned outage time, i.e. the available (except for planned outage time) cycle length. Hence L_A is given as:

$$L_A \equiv \frac{T_C - T_{RO} - T_{FO}}{T_C - T_{RO}} \qquad (29)$$

and L_C is given as equation 19. Combining equations 18c, 29 and 19, we can solve for T_A to obtain:

$$T_A = T_C - T_{RO} - T_I \left[\frac{T_C}{T_C - T_{RO} - T_{FO}} \right] + T_I \left[\frac{T_{RO}}{T_C - T_{RO} - T_{FO}} \right] \qquad (30)$$

Now from equation 28b $\qquad T_{CB} = T_C - T_I \left[\frac{T_C}{T_C - T_{RO} - T_{FO}} \right]$

we obtain from subtracting equation 30 from equation 28b

$$T_{CB} - T_A = T_{RO} - T_I \left[\frac{T_{RO}}{T_C - T_{RO} - T_{FO}} \right] = T_{RO} - T_I^{**} \qquad (31)$$

Finally the difference between T_A and EFPP is obtained by expressing EFPP from equation 6 now as

$$EFPP = L_A T_A$$
$$\qquad (18d)$$

Hence

$$T_A - EFPP = T_A (1 - L_A) \qquad (32)$$

Applying equations 30 and 29, we obtain

$$T_A - EFPP = \left[T_C - T_{RO} - T_I \left[\frac{T_C}{T_C - T_{RO} - T_{FO}} \right] + T_I \left[\frac{T_{RO}}{T_C - T_{RO} - T_{FO}} \right] \right] \frac{T_{FO}}{T_C - T_{RO}} \qquad (33a)$$

$$= T_{FO} - T_I \left[\frac{T_{FO}}{T_C - T_{RO} - T_{FO}} \right] = T_{FO} - T_I^{***} \qquad (33b)$$

21

Having now obtained these time differences,

$$T_C - T_{CB} = T_I^*$$ (34a)

$$T_{CB} - T_A = T_{RO} - T_I^{**}$$ (34b)

$$T_A - EFPP = T_{FO} - T_I^{***}$$ (34c)

we display them on Figure 10 which is an amplification of Figure 8. As a proof, note that the difference $T_C - EFPP$ should be (still assuming T_{MO} and T_{EO} are zero)

$$T_C - EFPP = T_I + T_{RO} + T_{FO}$$

This result does follow by summing equations 34a, 34b, and 34c as follows:

$$\begin{aligned}
T_C - EFPP &= T_C - T_{CB} + T_{CB} - T_A + T_A - EFPP \\[2mm]
&= T_I^* + T_{RO} - T_I^{**} + T_{FO} - T_I^{***} \\[2mm]
&= T_I\left[\frac{T_C}{T_C - T_{RO} - T_{FO}}\right] + T_{RO} - T_I\left[\frac{T_{RO}}{T_C - T_{RO} - T_{FO}}\right] + T_{FO} - T_I\left[\frac{T_{FO}}{T_C - T_{RO} - T_{FO}}\right] \\[2mm]
&= T_I + T_{RO} + T_{FO} \quad (QED)
\end{aligned} \tag{35}$$

Of course this result can be generalized to

$$T_C - T_{EFPP} = T_I + T_{PO} + T_{UO}$$

when T_{EO} and T_{MO} are not taken as zero.

Figure 10   Plant Operating Characteristics
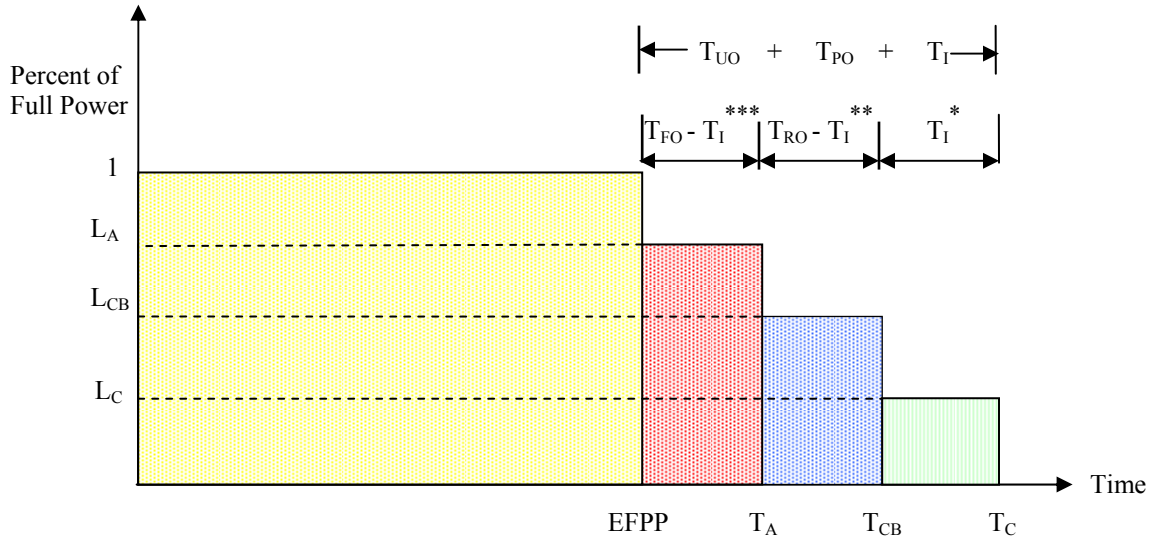
2.4 Plant Thermodynamic Efficiency, η

The core averaged outlet temperature and selected power conversion cycle are the prime determinants of achievable plant thermodynamic efficiency. For single phase liquid coolant the vapor pressure – temperature characteristic of the coolant primarily sets the outlet temperature within pressure limits that yield tolerable primary system boundary wall thickness (PWR) or if the boiling point is very high as for sodium, the outlet temperature is established to keep the primary system material boundary primarily in the elastic range (Sodium Fast Reactor). For a two phase coolant the outlet temperature is set by the selection of operating pressure which is selected to optimize critical power performance (BWR). For gas coolants, the outlet temperature is controlled by achievable performance of fuel and structural materials (HTGR).

Selection of the power conversion cycle is typically between a Rankine or a Brayton cycle. Both helium and supercritical carbon dioxide working fluids are specified in Brayton cycles. The PWR and BWR employ indirect and direct Rankine cycles respectively. The three fast reactors in the Generation IV program are evaluating indirect cycles of both the Rankine and Brayton types as well as direct versions of the latter.   The various high temperature gas reactor concepts under design specify both indirect and direct Brayton cycles.

Figure 11 illustrates the achievable plant efficiencies for various reactor types and power conversion cycles as outlet temperature is varied. Temperature ranges for hydrogen production processes under study are also included.
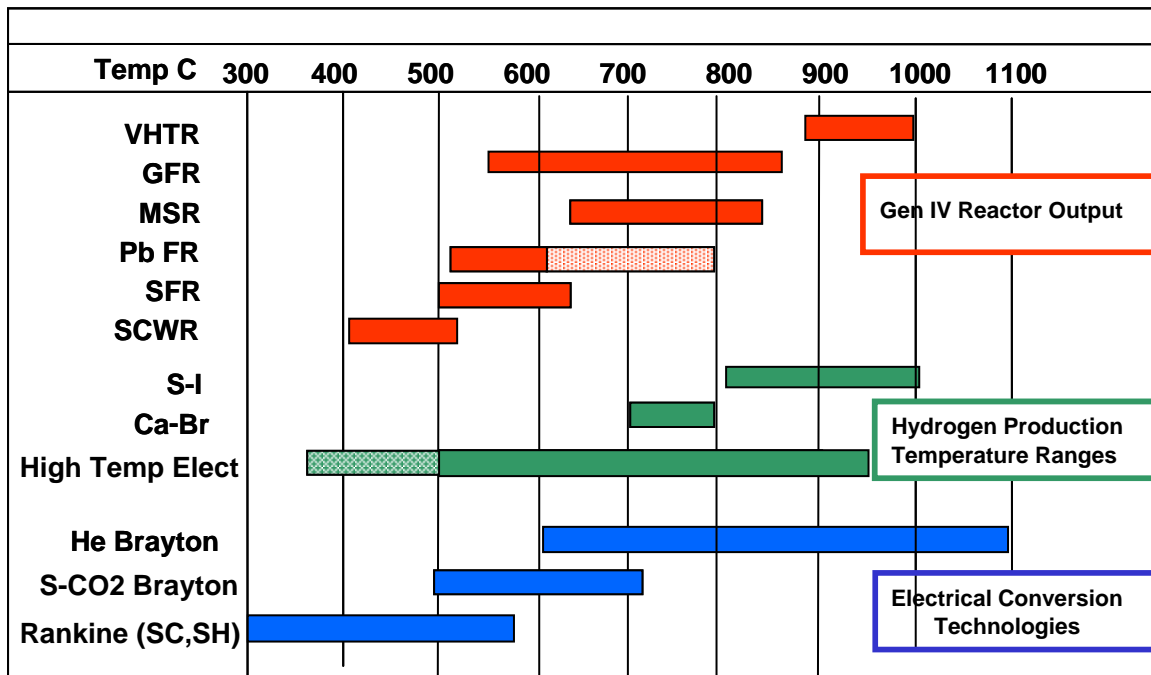
Figure 11. Generation IV Energy Conversion (from Picard, 2004)

2.5 Specific Power, q$_{sp}$

Specific power is a key parameter with respect to fuel cycle cost. For the typical PWR with specific power of $38 \; \dfrac{kW_{th}}{kg_{HM}}$, fuel cycle cost is about $5 \dfrac{mills}{kW-hre}$. Many other thermal parameters of design interest are related to specific power. These relationships are presented next.

2.5.1 Power Density, q_{PD}

Power density is the measure of the energy generated relative to the core volume. Because the size of the reactor vessel and hence the capital cost are nominally relative to the core size, the power density is an indicator of the capital cost of a concept. For propulsion reactors, where weight and hence size are a premium, power density is a relevant figure of merit.
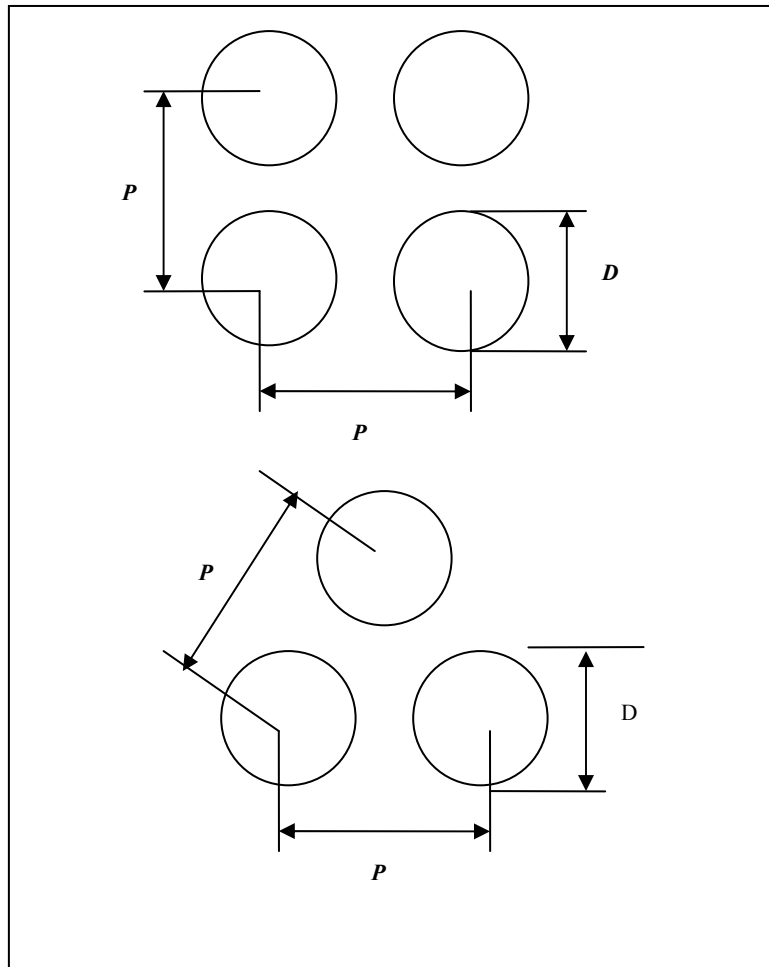
Figure 12. Square and triangular rod arrays

The power density can be varied by changing the fuel pin arrangement in the core. For an infinite square array, shown in Fig. 12, the power density q_{PD} is related to the array pitch, P, as:

$$q_{PD-square\ array} = \frac{4(1/4\pi R_{fo}^{2})q'''dz}{P^{2}dz} = \frac{q'}{P^{2}}$$

(36)

where

q'	Linear energy generation rate	$\dfrac{kWth}{m}$
q'''	Volumetric energy generation	$\dfrac{kWth}{cm^{3}}$
R_{fo}	Fuel pellet radius	mm

whereas for an infinite triangular array, the comparable result is:

$$q_{PD-triangular\ array} = \frac{3(1/6\pi R_{fo}{}^2)q'''dz}{\dfrac{P}{2}\left(\dfrac{\sqrt{3}}{2}P\right)dz} = \frac{q'}{\dfrac{\sqrt{3}}{2}P^2} \tag{37}$$

Comparing Eq. 36 and 37, we observe that the power density of a triangular array is 15.5% greater than that of a square array for a given pitch. For this reason, reactor concepts such as the LMFBR adopt triangular arrays, which are more complicated mechanically than square arrays. For light water reactors, on the other hand, the simpler square array is more desirable, as the necessary neutron moderation can be provided by the looser-packed square array [††].

The relationship between core average power density and specific power is

$$q_{PD} = \frac{q_{sp} \cdot M_{HM}}{V_{CORE}}$$

$$\left(\frac{kW}{l_{CORE}}\right) = \frac{\left(kW\Big/kg_{HM}\right)\cdot\left(kg_{HM}\right)}{l_{CORE}} \tag{38a}$$

Hence

$$q_{PD} = q_{sp}\rho_{HM}v_f \tag{38b}$$

where

q_{PD}	*core averaged power density*	$\dfrac{kWth}{l_{core}}$
ρ_{HM}	*heavy metal density in the fuel compound*	$\dfrac{kg_{HM}}{l_{fuel}}$
v_f	*volume fraction of fuel in the core*	l_{fuel}/l_{core}

Values of these parameters for a typical PWR and a conventional pin-type GFR core are given in Table 6.

[††] The Russian VVER fuel assembly is the exception being a triangular array of fuel pins with annular pellets with the same pin diameter (9.1 mm) and pitch (12.75 mm) as the advanced Westinghouse square array VVANTAGE 6 fuel assembly.

Table 6. PWR and GFR core parameters

Parameter	PWR	GFR
Specific Power [$kW_{th}/kg\ _{HM}$]	38	38
Core Power Density [kW_{th}/l_{core}]	104.5	100
Heavy Metal Density in fuel compound [$kg\ _{HM}/l_{fuel}$]	9.67	10
Volume Fraction of Fuel in the Core [$l_{fuel}\ /l_{core}$]	0.285	0.3

2.5.2   Linear Power

The relation between linear power and specific power is (for pin-type cores)

$$q' = q_{sp}\rho_{HM}\frac{\pi\ D^2_{\ pellet}}{4}(10^{-6})$$
(39)

where

q'	*linear power*	$\dfrac{kWth}{m}$
ρ_{HM}	*heavy metal density in fuel compound*	$\dfrac{kg_{HM}}{m^3}$
D_{pellet}	*pellet diameter*	*mm*

Figure 13 illustrates the relationship between the parameters of Equation 39 for UO_2[‡‡].

[‡‡] For UO_2 the theoretical density at room temperature is $10.97\text{x}10^3\ \dfrac{kg}{m^3}$. Since the weight fraction of U in

UO_2 is (238/(238+32)) ~ 88%, based on U-238 only, the U theoretical density is $9.67\ \text{x}10^3\ \dfrac{kg}{m^3}$
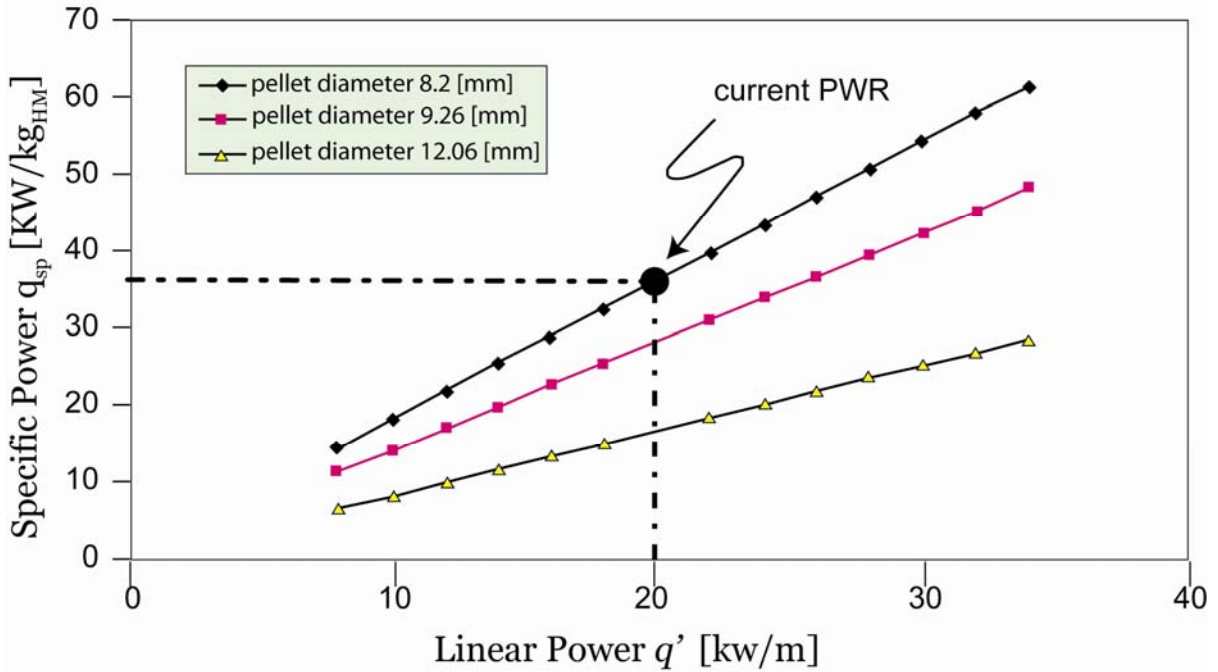
Figure 13. Linear Power - Specific Power Relationship (from Saccheri, 2002)

2.5.3   Heat Flux

The relations between heat flux (on outer rod surface) and specific power is (for pin-type cores)

$$q'' = q_{sp} \ \frac{\rho_{HM} \ \dfrac{\pi \ D_{pellet}^2}{4}}{\pi \ D} \left(10^{-3}\right)$$
(40)

where

q''	*heat flux on outer rod surface*	$\dfrac{kWth}{m^2}$
D	*fuel rod diameter*	*mm*

Figure 14 illustrates the relationship between the parameters of Equation 40 for UO_2.
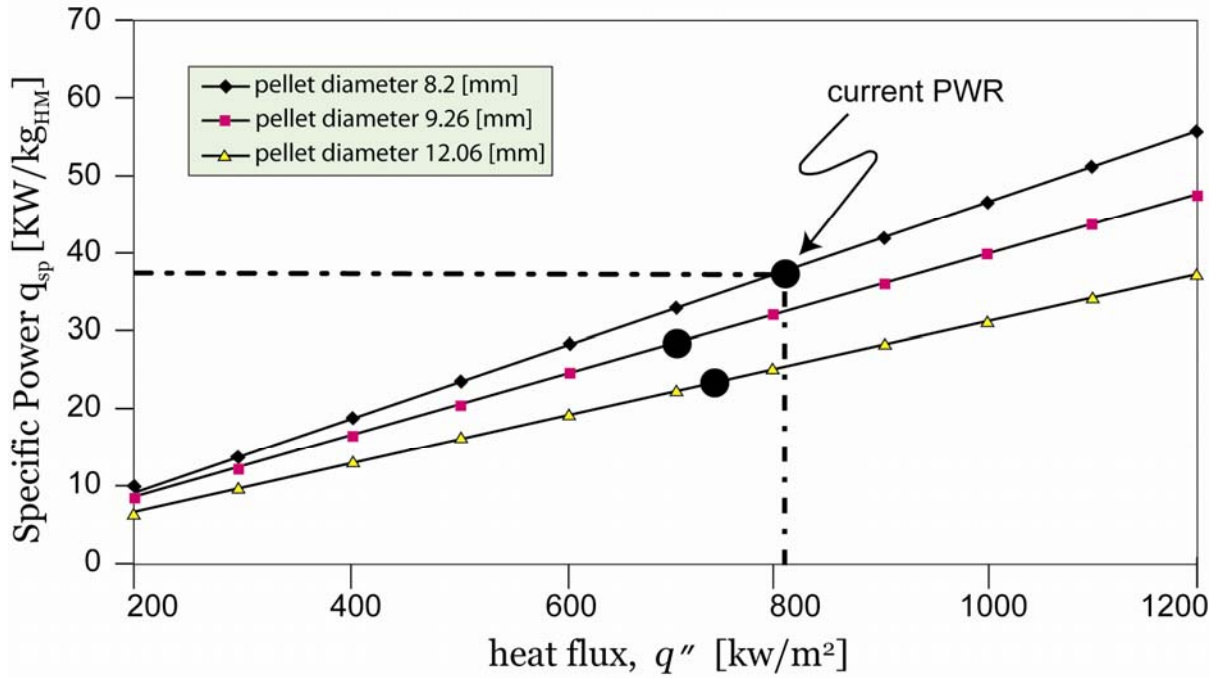
Figure 14. Heat flux - - Specific Power Relationship (from Saccheri, 2002)

2.5.4 Relations for Alternative Fuel Element Shapes

Let us compare the relations for inverted or matrix geometry to the pin geometry considered so far, following Williams 2003. Appendix D expands this comparison to other fuel shapes and parameters which dictate thermal performance in the GFR. Figure 15 illustrates these two geometries where each has been represented as a unit cell – hence, they will be called the matrix cell and the pin cell. Either can be established for square or triangular geometric arrays. The cell diameters are established by maintenance of consistent fuel cross-section (for the matrix cell) or coolant cross-section (for the pin cell) compared to the actual array. Hence for the square array

$$d_{cell} = \frac{2}{\sqrt{\pi}} P \tag{41}$$

while for the triangular array

$$d_{cell} = \sqrt{\frac{2\sqrt{3}}{\pi}} P \tag{42}$$

Note that these cell diameter formulae apply for the both matrix and pin cells. In the fuel pin literature these pin cells are known as the equivalent annulus approximation. The temperature fields for the coolant in the pin cell and the fuel in the matrix cell are accurate representation only for the sufficiently large P/D ratios, typically greater than *P/D = 1.2.*

For the matrix and pin cells the relevant geometric relationships are given in Table 7

Table 7.

	Symbol	Matrix Cell	Pin Cell
Equivalent gap thickness	t_g	d_g - d_{cl}	d_g - d_f
Clad thickness	t_c	d_{cl} - d_c	d_{cl} - d_g
Fuel bearing region volume fraction	v_{fb}	$\dfrac{d^2{}_{cell} - d^2{}_g}{d^2{}_{cell}}$	$\dfrac{d^2{}_f}{d^2{}_{cell}}$
Gap volume fraction	v_g	$\dfrac{d^2{}_g - d^2{}_{cl}}{d^2{}_{cell}}$	$\dfrac{d^2{}_g - d^2{}_f}{d^2{}_{cell}}$
Cladding volume fraction	v_{cl}	$\dfrac{d^2{}_{cl} - d^2{}_c}{d^2{}_{cell}}$	$\dfrac{d^2{}_{cl} - d^2{}_g}{d^2{}_{cell}}$
Coolant volume fraction	v_c	$\dfrac{d^2{}_c}{d^2{}_{cell}}$	$\dfrac{d^2{}_{cell} - d^2{}_{cl}}{d^2{}_{cell}}$
Volume fraction summation		$v_{fb} + v_g + v_{cl} + v_c = 1$	

The relevant thermal performance parameters are given in Table 8:

Table 8

	Matrix Cell	Pin Cell
q'	$q'''_{cell} \dfrac{\pi}{4} d^2{}_{cell}$	
q''	$\dfrac{q'}{\pi\, d_c} = \dfrac{q'''_{cell} d^2{}_{cell}}{4 d_c}$	$\dfrac{q'}{\pi\, d_{cl}} = \dfrac{q'''_{cell} d^2{}_{cell}}{4 d_{cl}}$
sp	$\dfrac{q'''_{cell}}{v_{fb} v_f f_f f_{HM} \rho_f}$ $\dfrac{q'''_{fb}}{v_f f_f f_{HM} \rho_f}$	

Example:

Let us illustrate pin cell and matrix cell performance for an assumed set of conditions for uranium carbide fuel.

Geometry	Fuel Properties	Operation Condition
$d_{cell} = 2.214 cm$	$\rho_f = 13\ g/cm^3$	$q'''_{cell} = 50\ W/cm^3$
$t_g = 0.005 cm$	$f_f = 0.94$	
$t_{cl} = 0.038$	$f_{HM} = 0.952\ g_{HM}/g$	

Next establish the defining parameters, d_c, for the matrix-cell and d_f for the pin-cell. For the matrix cell take

$$d_c = 1.4\ cm$$

For the pin cell we consider both square and triangular arrays and obtain the pitch, P, and fuel diameter, d_f, from the geometry already established. Hence

$$P_{square} = \frac{\sqrt{\pi}}{2} d_{cell} = 1.962\ cm$$

$$P_{tri} = \frac{\sqrt{\pi}}{\sqrt{2\sqrt{3}}} d_{cell} = 2.108\ cm$$

The fuel diameter is established from the volume fraction summation since it is the only remaining unprescribed parameter i.e.

since $v_{fb} + v_g + v_{cl} + v_c = 1$ (43)

For the matrix and the pin cell, volume fractions from the given data are:

	Matrix Cell	Pin Cell
v_g	0.006	0.007
v_{cl}	0.044	0.051
v_c	0.400	0.401
v_{fb}	0.550	To be calculated next

Hence,
$$v_{fb} + 0.007 + 0.051 + 0.401 = 1$$ (44)

Consequently,
$$v_{fb} = 0.541$$

$$\text{and so } d_f = (v_{fb}d^2_{cell})^{1/2} = [(0.541)(2.214)^2] = 1.629 \ cm \qquad (45)$$

The performance characteristics for these geometries are given in Table 7. Note that these cells have been sized for the given q'''_{cell} operating condition so that q' is identical for each geometry. The parameters q'''_{fb} and q_{sp} differ for each geometry since the fuel bearing region fractions, v_{fb}, differ as shown above.

Table 9.

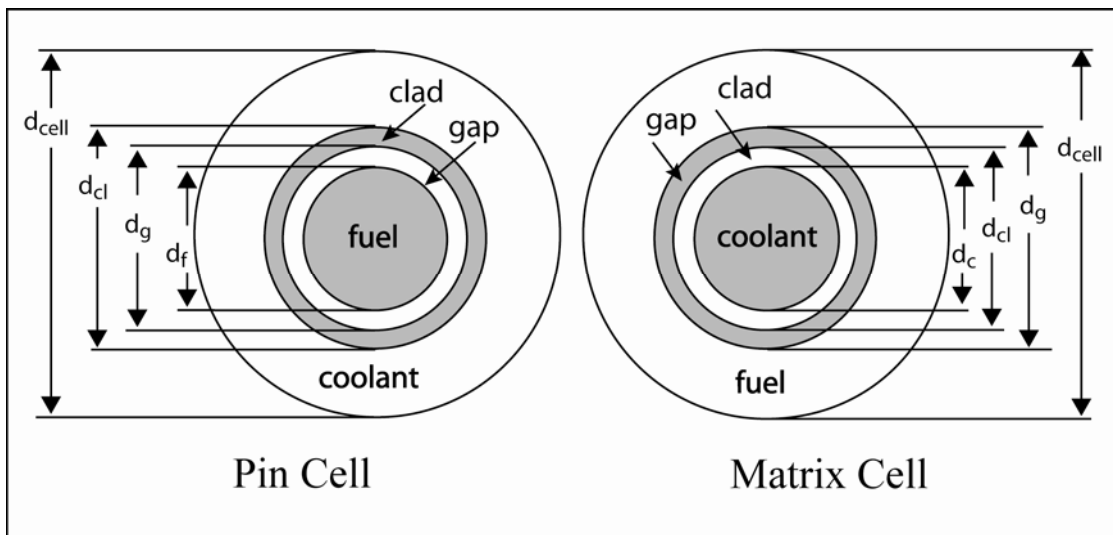| Equation	Matrix Cell	Pin Cell (Both Square and Triangular)
$q' = q'''_{cell} \dfrac{\pi}{4} d^2_{cell}$	19.25 kW/m	19.25 kW/m
$q'' = \dfrac{q'''_{cell}d^2_{cell}}{4d_c}$	43.8 W/cm^2	---
$q'' = \dfrac{q'''_{cell}d^2_{cell}}{4d_{cl}}$	---	35.7W/cm^2
$q'''_{fb} = \dfrac{q'''_{cell}}{v_{fb}}$	90.91 W/cm^3	92.42 W/cm^3
$q_{sp} = \dfrac{q'''_{cell}}{v_{fb}v_f f_f f_{HM}\rho_f} = \dfrac{q'''_{fb}}{v_f f_f f_{HM}\rho_f}$	19.54 kW/kg$_{HM}$	19.86 kW/kg$_{HM}$

Figure 15. Equivalent Annulus Representation of the pin cell geometry and the inverted or matrix cell geometry

32

VARIABLE	DEFINITION	UNITS

English Symbols

365.25	conversion factor	days/yr
8766	conversion factor	hrs/yr
Bu_c	operating cycle fuel burnup	$\dfrac{MW_{th}d}{kg_{HM}}$
Bu_d	fuel discharge burnup	$\dfrac{MW_{th}d}{kg_{HM}}$
Bu_1	Single batch (n=1) loaded core burnup	$\dfrac{MW_{th}d}{kg_{HM}}$
$\overline{c}_{lev}$	lifetime levelized unit COE	mills/ kW-hre
D_{pellet}	pellet diameter	mm
D	fuel rod diameter	mm
$EFPY$	effective full power years at fuel discharge	yrs
FOR	Forced outage rate	fraction
H/HM	Hydrogen to heavy metal atom ratio	dimensionless
q'	linear power linear energy generation rate	$\dfrac{kWth}{m}$
q''	heat flux	$\dfrac{kWth}{m^2}$
q'''	volumetric energy generation	$\dfrac{kWth}{cm^3}$
q_{PD}	core averaged power density	$\dfrac{kWth}{l_{core}}$
q_{sp}	specific power	$\dfrac{kWth}{kg_{HM}}$
Q_e	core electric power	kWe
Q_{th}	core thermal power	kWth
L	plant capacity factor (average fraction of rated full power achieved)	hrs operation/hrs total

L'	availability (accounts for time down due to forced outages only)	fraction
M_{Matrix}	Molecular Weight of Fuel Matrix ($ZrH_{1.6}$)	kg/kmol
M_{H2O}	Molecular Weight of Water	kg/kmol
M_{HM}	heavy metal mass	kg_{HM}
n	Number of batches	dimensionless
P	Pitch	mm
R_{FO}	Fuel pellet radius	mm
T_{AV}	available cycle length	yrs
T_c	operating cycle length (time between successive plant startups) or refueling interval	yrs /cycle
T_{fo}	forced outage length per cycle	days
T_{plant}	plant life	yrs
T_{res}	fuel in core residence time	yrs
T_{RO}	refueling outage length per cycle	days
V	Volume	mm^3
w	Weight fraction heavy metal	dimensionless
X	Number of Hydrogen Atoms Per Unit of the Fuel Matrix Element	dimensionless
Y	Number of Heavy Metal Atoms Per Unit of the Fuel Matrix Element	dimensionless
z	position	mm

Greek Symbols

$\in$	Enrichment (% U_{235})	%
η	plant thermal efficiency	kWe/kWth
ρ_{fuel}	Density of the Fuel	g/cm^3
ρ_{H2O}	Density of Water (at 700 F)	g/cm^3
ρ_{HM}	heavy metal density in the fuel compound	$\dfrac{kg_{HM}}{l_{fuel}}$ or $\dfrac{kg_{HM}}{m^3}$
v_f	volume fraction of fuel in the core	l_{fuel}/l_{core}

REFERENCES

1. Driscoll, M.J., Chapter 5 from "**Sustainable Energy - Choosing Among Options**" by Jefferson W. Tester, Elisabeth M. Drake, Michael W. Golay, Michael J. Driscoll, and William A. Peters. MIT Press, June 2005

2. Driscoll M.J., T.J Downar, E.E. Pilat, **"The Linear Reactivity Model for Nuclear Fuel Management"**, American Nuclear Society, 1990

3. GFR023, **"Development of Generation IV Advanced Gas-Cooled Reactors with Hardened/Fast Neutron",** System Design Report, International Nuclear Energy Research Initiative #2001-002F, February 2005

4. Driscoll M.J, P. Hejzlar, N. Todreas, "**Fuel-In-Thimble GCFR Concepts for GEN-IV Service**", Presented at ICAPP, Track 1135, Hollywood, FL, June 2002.

5. Handwerk, C.S., M.J. Driscoll, N.E. Todreas and M.V. McMahon, "**Economic Analysis of Implementing a Four-Year Extended Operating Cycle in Existing PWRs**", MIT-ANP-TR-049, January 1997

6. Picard, P. Figure 7, Personal Communication with N. Todreas, Fall 2004

7. Romano A., et al "**Implications of Alternative Strategies for Actinide Management in Nuclear Reactors**", Submitted to NSE, March 2005

8. Saccheri, J.G.B. and N.E. Todreas, "**Core Design Strategy for Long-Life, Epithermal, Water-Cooled Reactors",** MIT-NFC-TR-047 (July 2002).

9. Saccheri, J.G.B., N.E. Todreas, and M.J. Driscoll, "**A Tight Lattice, Epithermal Core Design for the Integral PWR",** MIT-ANP-TR-097 (August 2003).

10. Shuffler, C. **"Optimization of Hydride Fueled Pressurized Water Reactor Cores"**, M. S. Thesis, Department of Nuclear Engineering, Massachusetts Institute of Technology, September, 2004

11. Wang, D., M.S. Kazimi, and M.J. Driscoll, "**Optimization of a Heterogeneous Thorium-Uranium Core Design for Pressurized Water Reactors",** MIT-NFC-TR-057 (July 2003).

12. Williams, W., P. Hejzlar, M.J. Driscoll, W-J Lee and P. Saha, "**Analysis of a Convection Loop for GFR Post-LOCA Decay Heat Removal from a Block-Type Core**", MIT-ANP-TR-095, March 2003

13. Xu, Z. MJ. Driscoll and M.S. Kazimi, "**Design Strategies for Optimizing High Burnup Fuel in Pressurized Water Reactors**", MIT-NFC-TR-053, July 2003

APPENDIX A

Lifetime Levelized Cost Method (*Taken in the main from the M.S. Thesis of Carter Shuffler, Sept. 2004, which was based on the PhD Thesis of Jacopo Saccheri, August, 2003)*

The basic equations relating discrete cash flows and levelized costs are presented in the following paragraphs.

In order to charge the correct price for service, a utility must first decide on the rate of return on investment, *r*, which is desired. The rate of return is also commonly called the discount rate, or nominal interest rate (as opposed to the economists' "real" or inflation-free rate). Discrete expenditures for fuel cycle, Operations and Maintenance (O & M), and capital costs are incurred at different times during the plant's life. To get the levelized cost, these expenditures are discounted back to a reference date, which is chosen to be the start of irradiation for the first fuel cycle (i.e., $t = 0$). Discounting all expenditures to this date with continuous compounding of interest yields the present value of all costs, PV_{costs}, and a relationship with the lifetime levelized cost, $\overline{C}_{lev}$.

$$PV_{costs} = \sum_N C_N \cdot e^{-rT_N} = \int_0^{T_{plant}} \overline{C}_{lev} \cdot e^{-rt} dt \equiv \overline{C}_{lev} \int_0^{T_{plant}} e^{-rt} dt$$

(4.1)

where,

PV_{cost}	present value of all costs	$
C_N	N^{th} discrete cash flow	$
T_N	time relative to the ref. date for the Nth discrete cash flow	yrs
$\overline{C}_{lev}$	lifetime levelized cost	$/yr
T_{plant}	plant life	yrs
r	rate of return	%/yr

In addition to the discount rate, an escalation rate, *g*, can be included for recurring cash flows to account for price increases with time. Rewriting equation (4.1) to include this cost escalation effect yields:

$$PV_{costs} = \sum_N C_N \cdot e^{-rT_N} = \sum_N C_o \cdot e^{gT_N} \cdot e^{-rT_N} = \overline{C}_{lev} \int_0^{T_{plant}} e^{-rt} dt \qquad (4.2)$$

where,

C_o	1st discrete cash flow at reference date	$
g	escalation plus inflation rate	%/yr

36

Integrating equation (4.2) with respect to time and solving for the lifetime levelized cost yields:

$$\overline{C}_{lev} = PV_{costs} \cdot \left[\frac{r}{1 - e^{-rT_{plant}}} \right]$$ (4.3)

where,

$$capital\ recovery\ factor\ = \left[\frac{r}{1 - e^{-rT_{plant}}} \right]$$ (4.4)

The capital recovery factor, or carrying charge rate, relates the lifetime levelized cost of electricity, $\overline{C}_{lev}$, to the present value of all expenditures. It correctly accounts for the time value of money at the desired rate of return on investment. The lifetime levelized unit cost of electricity, $\overline{c}_{lev}$, is obtained by normalizing $\overline{C}_{lev}$ by the energy production from the plant, i.e. the equivalent of present-worthing the constant revenue stream $\overline{C}_{lev}$. If energy production is assumed to occur at a uniform rate over time, the lifetime levelized unit cost is the levelized cost ($/yr) divided by the annual energy production (kW-hre/yr). The annual energy production, E_{annual}, from the plant is:

$$E_{annual} = \dot{Q}_{th} \cdot \eta \cdot L \cdot 8766$$ (4.5)

where,

E_{annual}	annual energy production	kW-hre/yr
Q_{th}	core thermal power	kWth
η	plant thermal efficiency	kWe/kWth
L	plant capacity factor (average	
	fraction of rated full power achieved)	hrs operation/hrs total
8.766	conversion factor	hrs/yr x 10^{-3}

The final relationship for the lifetime levelized unit cost of electricity is given by the quotient of equations (4.3) and (4.5):

$$\overline{c}_{lev} = \frac{\overline{C}_{lev}}{E_{annual}} = \frac{PV_{costs}}{\dot{Q}_{th} \cdot \eta \cdot L \cdot 8.766} \cdot \left[\frac{r}{1 - e^{-rT_{plant}}} \right]$$ (4.6a)

where:

$\overline{c}_{lev}$	lifetime levelized unit COE	mills/kW-hrs
$\overline{C}_{lev}$	lifetime levelized COE	$/yr

37

If, as above, costs and the power are recorded in $ and kW_{th}, and for continuous interest rates (yr^{-1}), then equation (4.6) reports the levelized unit COE in mills/kW-hre, the desired units for the typical analysis. To get the individual levelized unit costs for the fuel cycle, O & M, and capital components, equation (4.6) is applied with the relevant cash flow histories incorporated into the PV_{costs} term. The levelized unit COE is simply the sum of the cost contributions from these individual components.

$$\overline{c}_{lev} = \overline{c}_{lev-fcc} + \overline{c}_{lev-O\&M} + \overline{c}_{lev-cap} \tag{4.7}$$

Alternate forms of Equation 4.6 of later use are obtained by manipulation if the energy production term. Specifically first maintain the energy production as annual but introduce specific power as a parameter yielding.

$$E_{annual} = q_{sp} \cdot M_{HM} \cdot \eta \cdot L \cdot 8.766 \tag{A}$$

where,

q_{sp}	specific power	$\dfrac{kWth}{kg_{HM}}$
M_{HM}	heavy metal mass	kg_{HM}

And second re-express energy production as the total produced over the plant lifetime.

$$E_{total} = q_{sp} \cdot M_{HM} \cdot \eta \cdot L \cdot 8.766 \cdot T_{plant} \qquad \text{kW-hre} \tag{B}$$

In the latter case Equation 4.6 is re-expressed as

$$\overline{c}_{lev} = \frac{\overline{C}_{lev} T_{plant}}{E_{total}} = \frac{PV_{costs}}{q_{sp} \cdot M_{HM} \cdot \eta \cdot L \cdot 8.766 \cdot T_{plant}} \cdot \left[\frac{rT_{plant}}{1 - e^{-rT_{plant}}} \right] \approx \left[1 + \frac{rT_{plant}}{2} \right] \tag{C}$$

or putting present value costs on a unit mass basis $/$kg_{HM}$ we obtain:

$$\overline{c}_{level} = \frac{\overline{C}_{lev} T_{plant}}{E_{total}} = \frac{C}{q_{sp} \cdot \eta \cdot L \cdot 8.766 \cdot T_{plant}} \cdot \left[\frac{rT_{plant}}{1 - e^{-rT_{plant}}} \right] \tag{4.6b}$$

where:

C	unit present value costs	$/$kg_{HM}$

Note that $\left[\dfrac{rT_{plant}}{1 - e^{-rT_{plant}}} \right] \approx \left[1 + \dfrac{rT_{plant}}{2} \right]$, which links equation (C) to equation (3a) of the text.

Further since fuel discharge burnup can be expressed in the denominator of Eqn. 4.6b as

$$Bu_d = 0.365 q_{sp} \cdot L \cdot T_c \qquad\qquad (D)$$

where:

Bu_d *fuel discharge burnup* $\dfrac{MW_{th}d}{kg_{HM}}$

0.365 *conversion factor* $\dfrac{daysMW_{th}}{yearW_{th}}$

Hence we can also express $\bar{c}_{level}$ as:

$$\bar{c}_{level} = \frac{C}{24.016 \cdot \eta \cdot Bu_d} \cdot \left[\frac{rT_c}{1 - e^{-rT_{plant}}} \right] \qquad\qquad (4.6c)$$

The alternate forms of 4.6 are individually useful for evaluation of the individual components of $\bar{c}_{lev}$.

The determination of PV_{costs} for each of the three cost components, i.e. PV_{fcc}, PV_{O+M} and PV_{cap} is the central task of the economic analysis of the cost of electricity for a reactor system. For examples of such analyses see Saccheri, 2003 for the IRIS reactor, Shuffler, 2004 for a zirconium hydride fueled PWR and Wang, 2003 for the gas fast reactor. For our purposes it is important to point out the design variables which these PV costs introduce.

For the fuel cycle costs the present value cost, PV_{fcc}, depends on the cash histories for all operating cycles over the lifetime of the plant. This leads to the following relations taking the reference date as the start of irradiation of the first operating cycle

$$PV_{fcc} = PV_{fccv,o} + \sum_{n=1} \cdot PV_{fccv,n} \cdot e^{-n \cdot r \cdot T_C} \qquad\qquad (4.42)$$

where:

$$PV_{fccv,o} = PV(UC_{fcc,o}) \cdot M_{HM} \qquad\qquad (4.40)$$

$$PV_{fcc,n} = PV_{fccv,o} \cdot e^{n \cdot g \cdot T_C} \qquad\qquad (4.43)$$

and new parameter definition are:

PV_{fcc}	*total present value of fuel cycle costs*	$
$PV_{fccv,o}$	*present value for the first operating cycle*	$
$PV(UC_{fcc,o})$	*present value unit cost for the first operating cycle*	$/kg_{HM}$
M_{HM}	*mass of heavy metal in the core*	kg
T_c	*operating cycle length*	years/cycle
	(time between successive plant startups)	

For the operations and maintenance costs the PV_{O+M} similarly depends on O+M expenditures over the plant life. Hence we have:

$$PV_{O\&M} = \sum_{n=0} CF_{O\&M,n} \cdot e^{-r \cdot (n+1)} \qquad (4.51)$$

where,

$$CF_{O\&M,n} = CF_{O\&M,o} \cdot e^{g \cdot n} \qquad (4.50)$$

and new parameter definitions are:

PV_{O+M}	*total present value of O+M*	$
	expenditure over plant life	
$CF_{O\&M,n}$	*n^{th} successive annual O+M expenditure*	$/yr
$CF_{O\&M,o}$	*total annual O+M expense*	$/yr
	for the first year of plant operation	

Finally, for capital costs, the PV_{cap} is the construction cost that occurs once during the plant lifetime. However, note that in actuality additional capital costs do take place in the life of a plant to accomplish major repairs, upgrades and the like.

Variable	Definition	Units
C	unit present value costs	$/ kg_{HM}
$\overline{C}_{lev}$	lifetime levelized COE	$/yr
C_N	N^{th} discrete cash flow	$
C_o	1st discrete cash flow at reference date	$
$CF_{O\&M,n}$	n^{th} successive annual O+M expenditure	$/yr
$CF_{O\&M,o}$	total annual of O+M expense for the first year of plant operation	$/yr
E_{annual}	annual energy production	kW-hre/yr
g	escalation rate	%/yr
PV_{cost}	present value of all costs	$
PV_{fcc}	total present value of fuel cycle costs	$
$PV_{fccv,o}$	present value for the first operating cycle	$
$PV(UC_{fcc,o})$	present value unit cost for the first operating cycle	$/ kg_{HM}
PV_{O+M}	total present value of O+M expenditure over plant life	$
r	rate of return	%/yr
T_N	time relative to the ref. date for the Nth discrete cash flow	yrs

Conversion Between Hydrogen/Heavy Metal and Pitch/Diameter Ratio (*Taken from M.S. Thesis of Carter Shuffler, September, 2004*)

The general notations for variables used in this derivation are defined in Table 8.1.

Table 8.1 General Nomenclature for Geometric Relationships for Square and Hexagonal Arrays

Name	Symbol	Units	Value UZrH$_{1.6}$	Value UO$_2$
Avogadro's Constant	N_A	atoms/kmol	6.02×10^{26}	6.02×10^{23}
Cladding Thickness	t_{cl}	mm	(2.14) & (2.16)	(2.14) & (2.16)
Density of the Fuel	ρ_{fuel}	kg/mm^3	8.256×10^{-6}	10.43×10^{-6}
Density of Water (at 700 F)	ρ_{H2O}	kg/mm^3	6.67×10^{-7}	6.67×10^{-7}
Diameter of Fuel Pellet	D_{pellet}	mm	(2.18)	(2.18)
Diameter of Fuel Rod	D	mm		
Gap Thickness	t_g	mm	(2.15) & (2.17)	(2.15) & (2.17)
Molecular Weight of Heavy Metal	M_{HM}	kg/kmol	237.85	237.85
Molecular Weight of Fuel Matrix (ZrH$_{1.6}$)	M_{Matrix}	kg/kmol	93.2	—
Molecular Weight of Water	M_{H2O}	kg/kmol	18	18
Number of Heavy Metal Atoms Per Unit of the Fuel Matrix Element	Y	dimensionless	1	1
Number of Heavy Metal Atoms	HM	dimensionless		
Number of Hydrogen Atoms Per Unit of the Fuel Matrix Element	X	dimensionless	1.6	—
Number of Hydrogen Atoms	H	dimensionless		
Pitch	P	mm		
Volume	V	mm^3		
Weight Percent Heavy Metal	w	fraction	0.45	0.8813

The number of hydrogen atoms in a prescribed volume of water and fuel (i.e. in a sub-channel/unit cell) is given by:

$$H = H_{H_2O} + H_{fuel} \tag{8.1}$$

where,

$$H_{H_2O} = 2 \cdot \frac{N_A \cdot \rho_{H_2O} \cdot V_{H_2O}}{M_{H_2O}} \tag{8.2}$$

$$H_{fuel} = X \cdot \frac{N_A \cdot \rho_{fuel} \cdot V_{fuel} \cdot (1-w)}{M_{Matrix}} \tag{8.3}$$

where,

X: number of hydrogen atoms per unit of the fuel matrix
w: weight fraction heavy metal in the fuel

Note that H_{fuel} is 0 for UO_2. The number of heavy metal atoms in a prescribed volume of fuel is given by:

$$HM = Y \cdot \frac{N_A \cdot \rho_{fuel} \cdot V_{fuel} \cdot w}{M_{HM}}$$
(8.4)

where,

Y: number of heavy metal atoms per unit of the fuel matrix

Taking the ratio of equations *(8.1)* to (8.4) gives the H/HM ratio:

$$\frac{H}{HM} = \left(\frac{2}{Y}\right) \cdot \left(\frac{1}{w}\right) \cdot \left(\frac{M_{HM}}{M_{H_2O}}\right) \cdot \left(\frac{\rho_{H_2O}}{\rho_{fuel}}\right) \cdot \left(\frac{V_{H_2O}}{V_{fuel}}\right) + \left(\frac{X}{Y}\right) \cdot \left(\frac{M_{HM}}{M_{Matrix}}\right) \cdot \left(\frac{1-w}{w}\right)$$
(8.5)

Since

$$wV_{fuel}\rho_{fuel} = V_{HM}\rho_{HM}$$

Then for UO_2 fuel for x = 0, y = 1, equation 8.5 reduces to equation 5 in the text.

Square Array

For square arrays,

$$V_{H_2O} = A_{flow-sq} \cdot L$$
(8.6)

$$V_{fuel} = A_{fuel} \cdot L$$
(8.7)

$$A_{flow-square} = P_{sq}^2 - \frac{\pi \cdot D^2}{4}$$
(8.8)

$$A_{fuel} = \frac{\pi \cdot D_{pellet}^2}{4}$$
(8.9)

To determine the diameter of the fuel pellet, the radial gap and cladding thicknesses must be specified. The original correlations for gap and cladding thickness used in [1] scaled linearly with rod diameter. It is believed by industry experts, however, that this leaves the gap and cladding too thin at small rod diameters. New correlations were therefore adopted that impose a minimum cladding and gap thickness.

if D_{rod} < 7.747 mm

t_{cl}= .508 mm
(8.10)

t_g = .0635 mm
(8.11)

if $D_{rod} > 7.747$ mm

$$t_{cl} = .508 + .0362 \cdot (D - 7.747) \ mm \tag{8.12}$$

$$t_g = .0635 + .0108 \cdot (D - 7.747) \ mm \tag{8.13}$$

$$D_{pellet} = D - 2 \cdot t_{cl} - 2 \cdot t_g \tag{8.14}$$

Substituting constants from Table 8.1 and equations (8.8) and (8.9) into equation (8.5) gives the H/HM ratios for square arrays of $UZrH_{1.6}$ and UO_2:

$$\left(\frac{H}{HM} \right)_{UZrH1.6} = 4.745 \cdot \left(\frac{\frac{4 \cdot P_{sq}^2}{\pi} - D^2}{D_{pellet}^2} \right) + 4.991 \tag{8.15}$$

$$\left(\frac{H}{HM} \right)_{UO2} = 1.918 \cdot \left(\frac{\frac{4 \cdot P_{sq}^2}{\pi} - D^2}{D_{pellet}^2} \right) \tag{8.16}$$

Rearranging and solving for P/D gives the desired relationship between the P/D and H/HM ratios:

$$\left(\frac{P}{D} \right)_{sq,UZrH1.6} = \sqrt{0.166 \cdot \left(\frac{D_{pellet}}{D} \right)^2 \left(\frac{H}{HM} - 4.991 \right) + 0.785} \tag{8.17}$$

$$\left(\frac{P}{D} \right)_{sq,UO2} = \sqrt{0.41 \cdot \left(\frac{D_{pellet}}{D} \right)^2 \left(\frac{H}{HM} \right) + 0.785} \tag{8.18}$$

Hexagonal Array

Equation (8.5) can also be applied to hexagonal arrays.

$$V_{H_2O} = A_{flow-hex} \cdot L \tag{8.19}$$

$$A_{flow-hex} = \frac{\sqrt{3} \cdot P_{hex}^2}{4} - \frac{\pi \cdot D^2}{8} \tag{8.20}$$

Substituting equations (8.19) and (8.20) and the constants in Table 8.1 into equation (8.5) gives the H/HM ratios for hexagonal arrays of $UZrH_{1.6}$ and UO_2:

$$\left(\frac{H}{HM}\right)_{UZrH1.6} = 4.745 \cdot \left(\frac{\dfrac{2 \cdot \sqrt{3} \cdot P_{hex}^2 - D^2}{\pi}}{D_{pellet}^2}\right) + 4.991 \qquad (8.21)$$

$$\left(\frac{H}{HM}\right)_{UO2} = 1.918 \cdot \left(\frac{\dfrac{2 \cdot \sqrt{3} \cdot P_{hex}^2 - D^2}{\pi}}{D_{pellet}^2}\right) \qquad (8.22)$$

Rearranging and solving for the P/D ratios gives:

$$\left(\frac{P}{D}\right)_{hex,UZrH1.6} = \sqrt{0.191 \cdot \left(\frac{D_{pellet}}{D}\right)^2 \cdot \left(\frac{H}{HM} - 4.991\right) + 0.907} \qquad (8.23)$$

$$\left(\frac{P}{D}\right)_{hex,UO2} = \sqrt{0.473 \cdot \left(\frac{D_{pellet}}{D}\right)^2 \cdot \left(\frac{H}{HM}\right) + 0.907} \qquad (8.24)$$

Thus it is shown that the P/D ratio depends on both the H/HM ratio and the rod diameter. The H/HM ratio is shown graphically in Figure 2.7 as a function of rod diameter and P/D ratio for square and hexagonal arrays of UZrH$_{1.6}$ and UO$_2$. Note that the rod diameter has very little influence on the H/HM ratio.

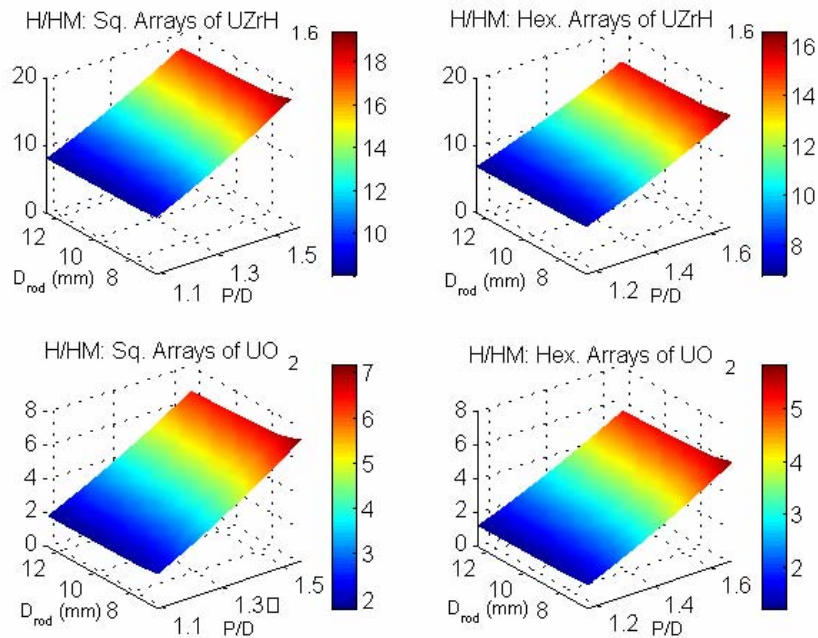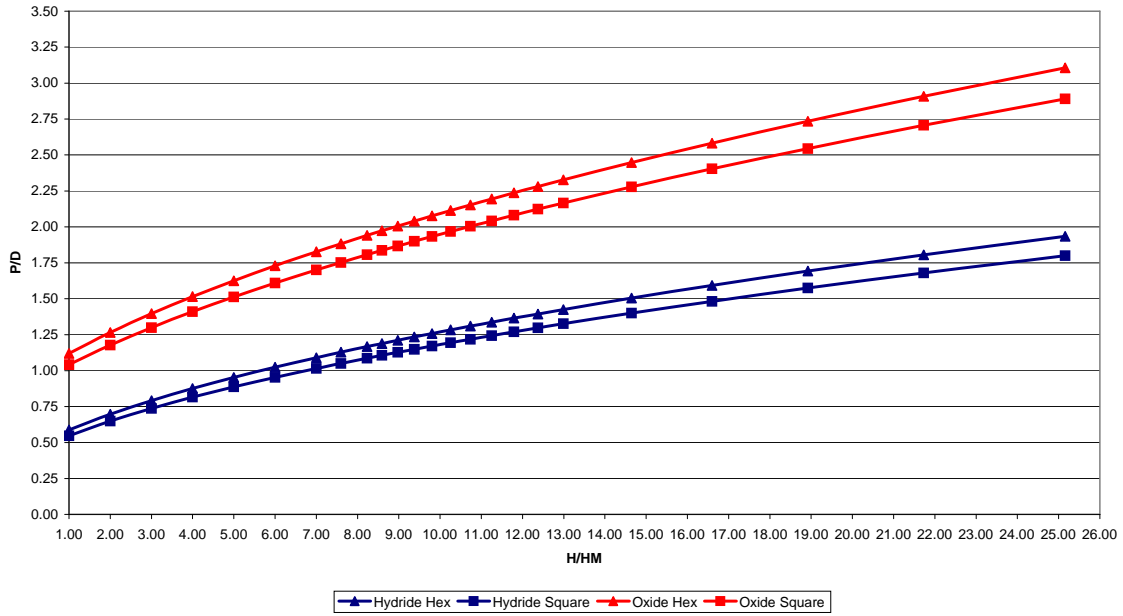**Figure 8.1a H/HM Ratio vs. P/D and D$_{rod}$ for Square and Hexagonal Arrays of UZrH$_{1.6}$ and O$_2$**

Figure 8.1b P/D vs H/HM for Square and Hexagonal arrays of UZrH$_{1.6}$ and UO$_2$

8.1.1.2 Relationship Between Square and Hexagonal Array Sub-Channels

To prove the geometric equivalence of square and hexagonal array sub-channels at the same rod diameter and H/HM ratio, a relationship between the square and hexagonal pitch is determined. This proof is only carried out for UZrH$_{1.6}$, but could easily be performed for UO$_2$ given the equations in Section 8.1.1.1.

For equivalent rod diameters and H/HM ratios, a constant C is defined such that,

$$C = \left(\frac{D_{pellet}}{D}\right)^2 \cdot \left(\frac{H}{HM} - 4.991\right) \qquad (8.25)$$

Substituting equation (8.25) into equations (8.17) and (8.23) gives the square and hexagonal P/D ratios for UZrH$_{1.6}$ with respect to C.

$$\left(\frac{P}{D}\right)_{sq,UZrH1.6} = \sqrt{0.166 \cdot C + 0.785} \qquad (8.26)$$

46

$$\left(\frac{P}{D}\right)_{hex,UZrH1.6} = \sqrt{0.191 \cdot C + 0.907} \tag{8.27}$$

Solving for P_{sq} and P_{hex}:

$$P_{sq} = D \cdot \sqrt{0.166 \cdot C + 0.785} \tag{8.28}$$

$$P_{hex} = D \cdot \sqrt{0.191 \cdot C + 0.907} \tag{8.29}$$

$$1.0746 \cdot P_{sq} = P_{hex} \tag{8.30}$$

For equivalent combinations of rod diameter and H/HM ratio, equation (8.30) can be used to relate the rod pitch between square and hexagonal lattices. This relationship also holds for UO_2, though the derivation is not provided.

The flow areas and heated and wetted perimeters are now presented for square and hexagonal arrays. Square and hexagonal unit cells are shown in Figure 8.2.

Figure 8.2 Square and Hexagonal Array Unit Cells
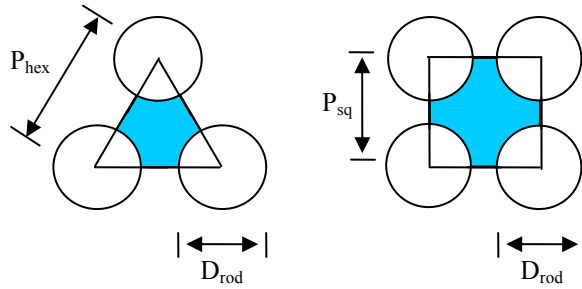
For the square array, the geometric relationships are:

$$A_{flow-sq} = P_{sq}^2 - \frac{\pi \cdot D^2}{4} \tag{8.31}$$

$$P_{w,sq} = P_{h,sq} = \pi \cdot D \tag{8.32}$$

The geometric relationships for the hexagonal sub-channel, with P_{hex} written with respect to P_{sq} according to equation (8.34), are:

47

$$A_{flow-hex} = \frac{\sqrt{3} \cdot (1.0746 \cdot P_{sq})^2}{4} - \frac{\pi \cdot D^2}{8} = 0.5 \cdot A_{flow-sq} \qquad (8.33)$$

$$P_{w,hex} = P_{h,hex} = \frac{\pi \cdot D}{2} = 0.5 \cdot P_{w,sq} = 0.5 \cdot P_{h,sq} \qquad (8.34)$$

The flow area and heated and wetted perimeters for the hexagonal sub-channel are exactly one half the corresponding values for the square sub-channel. They are identical, however, on a unit rod basis (hexagonal sub-channels have 0.5 rods and square sub-channels have 1 rod). Hence hexagonal and square designs with the same rod number, H/HM ratio, and rod diameter will have the same total flow area and heated and wetted perimeters.

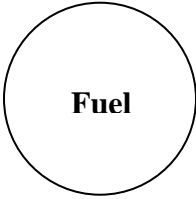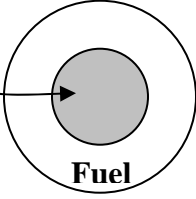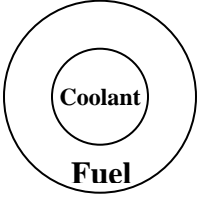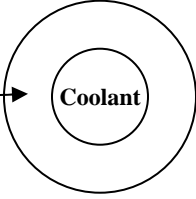## SUPPLEMENTAL NOMENCLATURE FOR APPENDIX B

Variable	*Definition*	*Units*
$EFPY_c$	*effective full power years of the operating cycle*	yrs

Appendix C
Comparative Performance Evaluation of Fuel Element Options *(Taken from Driscoll et al, 2002)*

Table II illustrates two additional fuel shapes compared to the pin and inverted or matrix cell geometries of Section 2.5.4. These were evaluated for GFR service (Driscoll, 2002)

TABLE II. Fuel Element Options

Configuration	Characteristics
Solid Pin (SP) **Coolant** **Fuel**	• Simplest, with broad experience base • Most common design choice
Annular, Externally Cooled Pin (AECP) **Ceramic Fiber in Void** → **Fuel** **Coolant**	• Can shorten or eliminate gas plenum at ends, reduce coolant ΔP
Annular, Externally and Internally Cooled Pin (AEIP) **Coolant** **Fuel** **Coolant**	• Reduces average and peak fuel temperature • Added cladding increases parasitic absorption • Fewer elements to fabricate per core • Can only radiate from outer surface after LOCA
Annular, Internally Cooled Matrix (AICM) **Fuel Within Matrix** → **Coolant**	• Matrix or added cladding absorbs and/or moderates neutrons • Increased energy storage capability • Topologically equivalent to annular internally cooled pin (AICP)

Three important features are summarized in Table III: gas film temperature difference, surface-to-peak temperature increase in the fuel, and unit cell volume (hence, number of elements in the core), all as a function of the key free variable, volume fraction fuel, selected on the basis of its dominant role in core neutronics; with implications as follows:

TABLE III. Scaling of Fuel Element Configurations[§§]

Element Type	Volume Fraction Fuel in Cell, ν_f	Cell Area, $\left(\dfrac{d_c}{d_h}\right)^2$	Fuel ℄ Temperature ΔT, $\left(\dfrac{16k}{sp\rho\, d_h^2}\right)\hat{\Delta T} =$	Gas Film ΔT, $\left(\dfrac{4h}{sp\rho\, d_h}\right)\Delta T_{gf} =$
Solid Pin (SP)	$\dfrac{1}{1+\left(\dfrac{d_h}{d_o}\right)}$	$\dfrac{\nu_f}{(1-\nu_f)^2}$	$\dfrac{\nu_f^2}{(1-\nu_f)^2}$	$\dfrac{\nu_f}{(1-\nu_f)}$
Annular Externally Cooled Pin (AECP)	$\dfrac{1-\left(\dfrac{d_i}{d_o}\right)^2}{\left[1+\left(\dfrac{d_h}{d_o}\right)\right]}$	$\dfrac{\nu_f\left[1-\left(\dfrac{d_i}{d_o}\right)^2\right]}{\left[1-\nu_f-\left(\dfrac{d_i}{d_o}\right)^2\right]^2}$	$\dfrac{\nu_f^2\left\{1-\left(\dfrac{d_i}{d_o}\right)^2\left[1-\ln\left(\dfrac{d_i}{d_o}\right)^2\right]\right\}}{\left[1-\nu_f-\left(\dfrac{d_i}{d_o}\right)^2\right]^2}$	$\dfrac{\nu_f\left[1-\left(\dfrac{d_i}{d_o}\right)^2\right]}{\left[1-\nu_f-\left(\dfrac{d_i}{d_o}\right)^2\right]}$
Annular Internally and Externally Cooled Pin (AEIP)	$1-\left(\dfrac{d_h}{d_o}\right)$ and $d_h = d_i$	$\dfrac{2-\nu_f}{(1-\nu_f)^2}$	$\sim \dfrac{\nu_f^2}{2(1-\nu_f)^2}$	$\dfrac{\nu_f}{(1-\nu_f)}$
Annular Internally Cooled Matrix (AICM)	$1-\left(\dfrac{d_h}{d_o}\right)^2$ and $d_h = d_i$	$\dfrac{1}{(1-\nu_f)}$	$\dfrac{-\ln(1-\nu_f)-\nu_f}{(1-\nu_f)}$	$\dfrac{\nu_f}{(1-\nu_f)}$

where d_o, d_i, d_h, d_c = outer fuel, inner fuel, hydraulic, and unit cell diameters. For square pitch, $P^2 = (\pi/4)d_c^2$; for triangular pitch, $P^2 = \left[\pi/(2\sqrt{3})\right]d_c^2$.

NOTE: For fixed sp, ρ and ν_f the total core volume, thermal and pumping power are the same. The number of elements in a core is inversely proportional to $(d_c/d_h)^2$ since d_h is fixed.

[§§] Also see Hankel "Stress and Temperature Distributions", Nucleonics, Vol. 18, No 11, Nov., 1960

<u>Column 1</u>, Fuel Volume Fraction, v_f.

Fuel volume fraction is important because high v_f favors good neutron economy (low parasitic absorption and leakage). Here it is expressed as a function of the hydraulic diameter of the coolant channels, d_h and the OD of the fuel pin, d_o. The hydraulic diameter is the single factor which best determines core thermal-hydraulic performance and would logically be held constant when comparing the four element options.

<u>Column 2</u>, Cell diameter squared is proportional to the area occupied by the unit cell in the horizontal plane.

It is shown here as a function of v_f (and for the annular pellet case, also as a function of the diameter of the central void, d_i). Its inverse is proportional to the number of fuel elements in a core of fixed volume and power.

<u>Column 3</u>, Maximum Radial Fuel Temperature Rise.

As can be seen from the column heading, ΔT also depends on the fuel thermal conductivity, k, and its power density, $q''' = sp\rho$, kW/m^3, where ρ is kg heavy metal per m^3 and sp the specific power, kW/kg. Holding this grouping (and as noted before, d_h) constant gives ΔT as a function of v_f.

<u>Column 4</u>, Gas Film (Surface-to-Bulk) Temperature Difference.

In addition to power density, $sp\rho$, ΔT_{gf} depends on the heat transfer coefficient, h, kW/m^2°C. When factored as shown, the ΔT_{gf} is also primarily a function of v_f.

Table IV gives values of the indices of Table III for 50 volume percent fuel—a representative design point for older GCFR cores.

From Tables III and IV one can draw several useful conclusions:

1. First of all (at fixed volume fraction fuel), one cannot reduce gas film ΔT compared to a solid pin. This is unfortunate because in a GCFR cladding temperature, and hence ΔT_{gf}, is the most restrictive constraint.

2. On the other hand, AEIP and AICM elements reduce peak fuel temperature. However, given our choice of

TABLE IV. Comparison of Fuel Types at 50 Vol.% Fuel

Type	Dimensions	Cell Area	Fuel ΔT	Film ΔT
SP	$\dfrac{d_h}{d_o} = 1$	2 (0.5)*	1	1
AECP	e.g., ** $\dfrac{d_h}{d_o} = 0.60$ $\left(\dfrac{d_i}{d_o}\right)^2 = 0.20$	4.44 (0.23)	1.33	1.33
AEIP	$\dfrac{d_h}{d_o} = 0.50$	6 (0.17)	0.50	1
AICM	$\dfrac{d_h}{d_o} = 0.71$	2 (0.5)	0.39	1

( )* = number of elements is proportional to this value, the inverse of cell area.

** note that there is no unique choice, different pairs can give the same v_f, however the trends are the same.

UO_2, this is not that helpful because specific power is limited to modest values by the clad temperature constraint.

3. The constraints applied in derivation of the entries in Table III also impose constant core volume, thermal and pumping power. Hence the larger cell volumes of annular fuel mean that fewer elements need be fabricated.